SBIR Phase II Final Scientific/Technical Report

DOE Award Number: DE-SC0013731

Sponsoring Program Office: Office of Science, Department of Energy

Name of Recipient: LCW Supercritical Technologies Corporation

Project Title: Production of Uranium from Seawater Using a Novel Polymer Adsorbent – Process Development and Cost Analysis

Principal Investigator: Dr. Chien M. Wai

Team Members: Dr. Horng-Bin Pan
Dr. Joanna S. Wang
Kevin Hutchison

Collaborators (PNNL– Marine and Coastal Research Laboratory)
Dr. Gary A. Gill
Dr. Li-Jung Kuo
Jonathan Strivens

Collaborators (Texas A&M University at Galveston)
Dr. Peter H. Santschi
Dr. Peng Lin
Dr. Chen Xu

Table of Contents

I. Background

Research in developing techniques for extracting uranium from seawater is of considerable current interest.[1-11] One reason which drives scientists to develop techniques of sequestering uranium from ocean is the prediction that the land-based uranium reserves would be depleted by the end of this century based on the current production rate.[1, 2] Uranium exists in seawater at a very low concentration (about 3 ppb) and as highly stable uranyl tris-carbonato complexes, primarily in the form $Ca_2[UO_2(CO_3)_3]$.[12] Because of the enormous volume of seawater, the total amount of uranium in ocean is estimated to be a thousand times greater than the land-based uranium resources.[1, 2] As early as 1964, the idea of extracting uranium from seawater was discussed by Davies et al. in a Nature paper.[13] In the past decades, many different materials were tested to evaluate their ability for sequestering uranium from seawater.[1, 2, 14, 15] Among them, amidoxime and carboxylate containing polymer fiber adsorbents appear most promising because of their high uranium adsorption capacity and stability in seawater. The carboxylate groups are necessary to make the polymer adsorbent hydrophilic whereas the amidoxime groups provide strong coordination sites for uranyl ions. Moreover, according to theoretical analysis, the adsorbability of uranium may involve synergistic effects of both amidoxime and carboxyl groups in the fiber adsorbent.[16]

Using radiation induced grafting techniques to produce amidoxime and carboxylate containing polymer fibers for extraction of uranium from seawater were extensively investigated by Japanese scientists for nearly 3 decades beginning in the 1990s. The efficiencies of uranium extraction from seawater using these materials were modest typically in the range of 0.5–4 grams of uranium per kilogram of fiber.[17] Recently, scientists at Oak Ridge National Laboratory (ORNL) synthesized a new type of high-surface-area polymer fibers with amidoxime and carboxylic acid functional groups using a radiation induced grafting technique.[18, 19] The method involves grafting of acrylonitrile and itaconic acid to a high-surface-area polyethylene fiber with high energy electrons followed by chemical conversion of the nitrile groups to amidoxime groups with hydroxylamine. The fiber adsorbent requires a KOH conditioning step to make it effective for uranium extraction from seawater. The ORNL adsorbent shows a uranium adsorption capacity of 4.48 grams uranium per kg of the polymer fiber after 56 days of exposure in a seawater flume system, which is higher than any previously reported uranium adsorption capacities of amidoxime-carboxylate containing fiber adsorbents.[19] The ORNL fiber also grabs other metals from seawater particularly vanadium which has a concentration factor an order of magnitude higher than that of uranium on a molar basis.[18-20] Vanadium appears to be a potential competing metal for sequestering uranium from seawater.[21-23] Several reports suggest that minimizing vanadium adsorption is one possible way of improving uranium extraction efficiency from seawater using this type of polymer adsorbents.[22-25]

Recent theoretical studies to evaluate the mechanisms of uranyl adsorption with amidoxime-based fibers were based on uranyl reactions with glutarimidedioxime (cyclic form) and glutardiamidoxime (open-chain) as model molecules.[26, 27] The cyclic glutarimidedioxime (a tridentate ligand) has received much attention because it has a greater binding constant with uranyl

ions relative to the open-chain glutardiamidoxime.[27] The conditions for synthesis of glutarimidedioxime and glutardiamidoxime by the reaction of hydroxylamine with glutaronitrile are different as shown in Scheme 1.[26, 27] To improve uranium extraction efficiency of the polymer fiber, many recent studies focused their efforts on formation of the cyclic structure of the amidoxime groups in the amidoximation process by reflux at elevated temperatures.[14, 18-20, 28-30] In a number of recent reports, polymer fibers containing mainly the cyclic imide-dioxime groups were utilized for extraction of uranium from seawater with good results.[18-20, 29, 30]

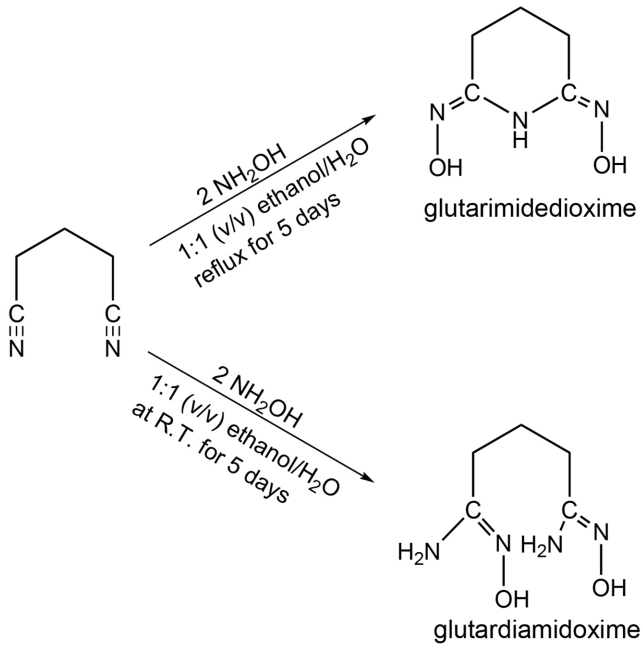

Scheme 1. Synthesis of glutardiamidoxime and glutarimidedioxime from glutaronitrile

A recent NMR study shows that pentavalent vanadium (Na_3VO_4) reacts effectively with the cyclic glutarimidedioxime in 0.5 M NaCl aqueous solutions (pH = 8.3) to form a 1:1 complex.[31] The branch-chain glutardiamidoxime molecule does not form any detectable complexes with vanadium ions in the NMR study[24, 31] and potentiometric titration experiments[24]. Abney and co-workers utilized X-ray absorption fine structure (XAFS) spectroscopy to investigate ORNL high-surface-area amidoxime-based fibers following deployment in natural seawater and revealed that vanadium was bound solely to the cyclic imide-dioxime.[24, 32] This appears consistent with the high vanadium extraction in previous uranium-from-seawater reports utilizing glutarimidedioxime dominated polymer fibers.[18-20, 29, 30] The stability constant of vanadium complex with glutarimidedioxime is extreme large ($\log \beta = 53.0 \pm 0.4$).[24] Because of the strong bonding, elution of vanadium from the amidoxime-based adsorbents is difficult. How to develop this type of chelating fibers with high uranium and low vanadium adsorption capabilities becomes an important question for further improvement of their seawater uranium extraction efficiencies for possible commercial applications.

Attempts of utilizing polyacrylonitrile (PAN) as a starting material to produce only amidoxime-containing polymer adsorbents for sequestering uranium from seawater were reported

in the literature.[28, 33, 34] This approach is attractive because PAN is commercially available in large quantities. However, the results of seawater tests of the amidoxime-containing adsorbent prepared from PAN were not impressive and further research effort in this direction was basically abandoned. We have recently examined the chemistry of converting nitrile groups in acrylic fiber to both amidoxime and carboxylate containing functional groups using ^{13}C CP/MAS solid-state NMR and vibrational spectroscopy to control amidoxime configuration and its ratio to carboxylate for optimizing uranium adsorption capacity. We found that conversion of nitrile groups to carboxylate groups in original acrylic fibers using 1 M NaOH does not proceed effectively. However, if a portion of the nitrile groups in the original acrylic fiber is already converted to amidoxime, further conversion of the nitrile groups to hydroxyl groups occurs effectively in 1 M NaOH at room temperature. The amidoxime group acts like a catalyst for the hydrolysis of nitrile to carboxylate in the fiber. Thus, acrylic fiber can be converted to amidoxime and carboxylate containing polymer fibers using a two-step sequential reaction process, i.e., amidoximation using hydroxylamine followed by carboxylation with NaOH as illustrated in Figure 1. The ratio of the two functional groups in the fiber can be monitored by FTIR spectroscopy. The fiber adsorbent prepared by this procedure has a gel-like property. However, when it is immersed in a salt solution such as seawater, it changes to a fiber-like material immediately and disperses nicely in flowing seawater. The details of our synthetic procedure and some key properties of the synthesized fiber including nature of the amidoxime groups and adsorption capacities of uranium and vanadium in seawater are described in the next section.

II. Synthesis and Characterization of Amidoxime-Carboxylate Containing Fiber

The acrylic fiber used initially in this investigation is common acrylic yarn (100% acrylic or Orlon) which is available from many fabric stores. The fiber is made of polyacrylonitrile with some ester copolymer (<15%). According to our preliminary experiments, even recycled yarn (100% acrylic) can be used as starting material for synthesizing the amidoxime-carboxylate containing fiber adsorbent. Long textile-grade acrylic fibers (92% acrylonitrile and 8% methyl acrylate monomers) from Kaltex were later used to make braids 20–25 cm in length for seawater flume tests. Our procedure of converting the acrylic fibers to amidoxime-carboxylate containing polymer adsorbents involves the following two steps:

1. Immerse the fibers in a 1:1 (v/v) methanol/water solution with 3% by weight of hydroxylamine (NH_2OH) at room temperature (about 21 ºC) for 1 hour and then heat the solution at 70 ºC for 45 minutes. FTIR spectra show that about 50% of the nitrile groups of the original acrylic fibers are converted to amidoxime groups. The treated fibers are washed with water several times for the next step of synthesis.
2. The washed fibers are placed in a sodium hydroxide (1 M NaOH) solution at room temperature (about 21 ºC) for 24 hours. The alkaline solution converts nitrile groups to carboxylate groups as shown in the FTIR spectra given in Figure 2. Conversion of nitriles to carboxylate is sufficient under the specified condition with a small fraction of the nitrile peak still detectable in the FTIR spectrum. The presence of some nitrile groups in the final

product contributes to the mechanical strength of the polymer adsorbent.[34-36] Without nitrile groups, the resulting fiber shows a more gel-like property.

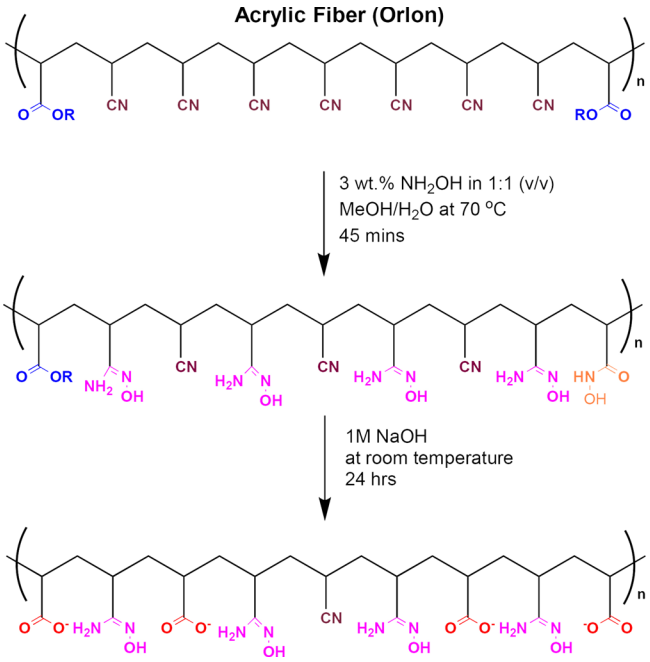

Figure 1. Conditions of the two-step conversion of acrylic fiber to amidoxime and carboxylate containing polymer adsorbent

The reaction conditions and the ratio of amidoxime to carboxylate groups in the final fiber adsorbent were determined by our initial bench scale experiments. Control of the functional groups in the fiber adsorbent was determined by FTIR spectroscopy (Figure 2). The ester group's –C=O stretching peak at 1736 cm^{-1} becomes barely detectable after the synthesis suggesting that most of the ester groups in the acrylic fiber are converted to carboxylate groups in the NaOH treatment step. Conversion of ester to carboxylate in alkaline solution is known to occur. Moreover, a broad C=O stretching band at around 1750 cm^{-1} indicates that a small amount of the carboxylate groups is converted to carboxylic acid groups (–COOH) during rinsing with deionized water. The fiber adsorbent was also characterized by solid-state ^{13}C NMR shown in Figure 3. The chemical shifts at 183 and 177 ppm are assigned to the carboxylate ($–COO^-$) and carboxylic acid (–COOH) group, respectively, consistent with the literature.[37] Ester is also known to react with hydroxylamine to form hydroxamic acid[38, 39] which may explain the change in the 1736 cm^{-1} peak after the amidoximation step. The hydroxamic acid group has a strong carbonyl absorption at about 1640 cm^{-1} [40, 41], a medium-intensity amide II band near 1550 cm^{-1}, and a N–O band at about 900 cm^{-1}.[40, 41] However, the three bands of the hydroxamic acid group overlap with amidoxime characteristic bands, C=N, N–H, and N–O, respectively.[40, 41] The final distribution of the chemical groups in the fiber adsorbent is estimated to be 46% amidoxime, 45% carboxylate, and 9% nitrile. Our method of estimating the amidoxime/COO^- ratio and –CN intensity in the fiber adsorbent is described in the Supplementary Information of a paper published in 2020.[42] The adsorbent so

prepared does not require KOH conditioning[11] because nitrile converts to carboxylate directly in 1 M NaOH at room temperature.

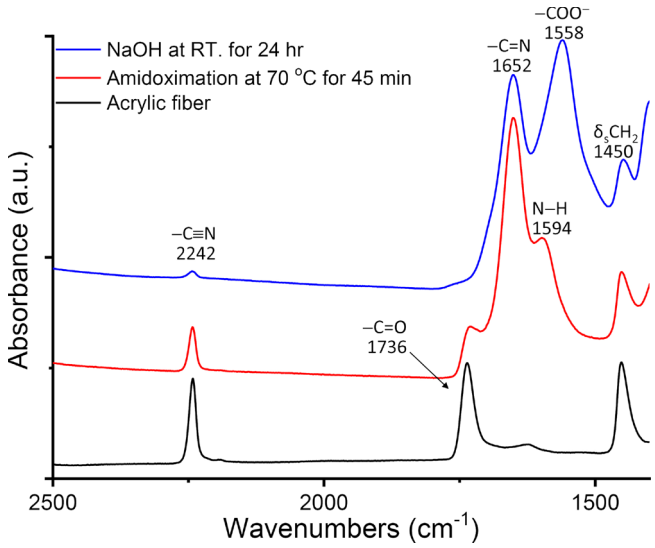

Figure 2. FTIR spectra of the original acrylic fiber (black), after amidoximation (step 1, red), and after NaOH treatment (step 2, blue). Conditions: Step 1, NH_2OH 70 °C 45 minutes; Step 2, NaOH room temperature 24 hours. (The spectra were normalized to the $–CH_2–$ in-plane bending or scissoring band ($\delta_s CH_2$) at 1450 cm^{-1})

When the amidoximation reaction is carried out at 70 °C for about 45 minutes, the product contains mainly the branch-chain diamidoxime groups which should reduce vanadium adsorption. A ^{13}C CP/MAS solid-state NMR spectrum of the fiber produced under the specified conditions is shown in Figure 3. For comparison, the ^{13}C CP/MAS solid-state NMR spectrum of an amidoxime-carboxylate containing fiber prepared by a radiation-induced grafting method is also given in the inset (green color) of Figure 3. This adsorbent contains mainly the cyclic imide-dioxime groups.[19]

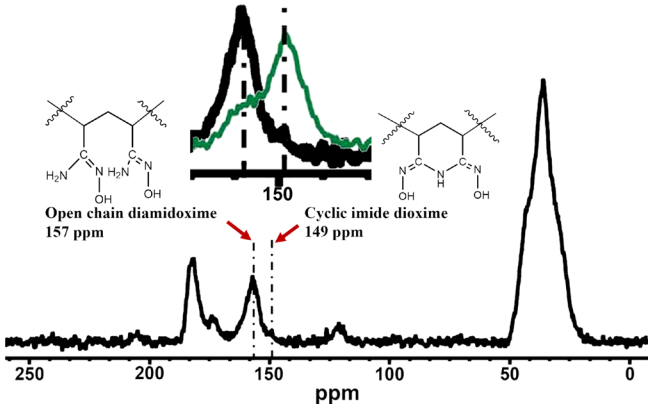

Figure 3. ^{13}C CP/MAS solid-state NMR spectrum of acrylic fiber after hydroxylamine reaction at 70 °C for 45 min. The green color spectrum on the inset is grafting produced amidoxime-containing fiber reported in the literature[19]. The signal at 157 ppm is assigned to acyclic

amidoxime accompanied by a relatively small shoulder at 149 ppm assigned to cyclic imide dioxime. The chemical shifts at 183 and 177 ppm are assigned to the carboxylate ($–COO^-$) and carboxylic acid (–COOH) groups, respectively.[37] A small signal observed at 121 ppm is assigned to the nitrile (C≡N) group. The huge broad peak at 36 ppm is assigned to the $–CH_2$ and –CH groups of the polymer backbone chain.

III. Scale-up Production of LCW Fiber Adsorbent

The fiber used for the scale-up synthesis is long textile grade acrylic fiber (approximately 5 meters in length and 20–25 microns diameter) manufactured by Grupo Kaltex in Mexico. The fibers were cut into different lengths to make braids of different weights. Initial syntheses were conducted using 15 grams of acrylic fiber in a 2-liter reactor (Figure 4). A key parameter to optimize is the ratio of mass of adsorbent to solution volume. The products were characterized by FTIR and tested for their uranium adsorption capacities in a seawater flume system at PNNL-MCRL located in Sequim, Washington. The optimal parameter obtained from the first scale-up process was then used to synthesis a 150-gram batch of LCW fiber adsorbent using a 20-liter reactor. Utilizing the 20-liter reactor, we could prepare about one kilograms of the amidoxime-carboxylate containing polymer fiber adsorbent (50 cm long) in four weeks (Figure 4). The fiber braids were tested for uranium adsorption from seawater at PNNL-MCRL (Marine and Coastal Research Laboratory) using a raceway flume system and found to perform similar to previous batches.

Figure 4. Left panel ― 4–6 g masses of adsorbent synthesized using a 2 L reaction vessel. Right Panel ― 50 cm long, 40–80 g braids synthesized using a 20 L reactor.

The scaling up of the adsorbent synthesis was expanded to a 50-liter reactor system with an external solution recirculation device (Figure 5a). This system was designed after the system used by Japanese scientists at the Takasaki Advanced Radiation Research Institute to synthesize amidoxime-based adsorbent material. A major limitation we identified at this scale was bubble formation on the surface of the fiber, which inhibited even and effective amidoximation. The 50-

liter reaction system was also found to have copper contamination probably from the pump recirculation system.

The most satisfactory system for large scale synthesis of the fiber adsorbent is using stainless steel sonication bath which can disperse the bubbles formed on fiber surfaces during the synthesis. Our preliminary small-scale synthesis of LCW fiber adsorbent using a 2-liter lab sonication bath was successful in removing gas bubbles from the fiber surface based on visual observation. Ultrasound tends to agitate the liquid, which not only makes the solution more homogeneous but also improves the dispersion of fiber in the solution. A 30 L stainless steel sonication bath (Figure 5b) placed in a hood was used for synthesis the fiber adsorbent for our scale up experiments. Larger sonication baths are available commercially, but they are too big for our hood to accommodate. The 30 L sonication bath can synthesis about 200 grams of fiber adsorbent in each batch in three days.

Figure 5. (a) 50 L recirculating reactor for preparation of fiber adsorbent; (b) 30 L Ultrasonic bath for LCW fiber adsorbent synthesis.

IV. Initial Marine Tests of Small Fiber Braids

IV-A. Seawater Exposure Systems

Initial marine testing was conducted at PNNL's Marine and Coastal Research Laboratory (MCRL), a coastal-based marine laboratory within PNNL, using ambient seawater from Sequim Bay, WA. The MCRL has a seawater delivery system that can provide ambient seawater into a "wet laboratory" for scientific investigations. Ambient seawater is drawn by pump from a depth of ~10 m from Sequim Bay through a plastic pipe. Raw seawater is pumped directly into the laboratory for use. Filtered seawater is obtained by first passing raw seawater through an Arkal Spin Klin™ filter system (nominal pore size 40 μm) to remove large particles. The partially filtered seawater is then stored in a large volume (~ 3,500 gal) reservoir tank outside the laboratory. This seawater is gravity fed into the laboratory research facilities through PVC piping where it can be passed through additional filtration to remove finer particles if needed at the point of use. Two types of exposure systems are employed in this program: (1) flow-through columns for testing

small amounts (~50 mg) of fiber materials and (2) recirculating seawater flumes for testing braided fiber adsorbent materials (~10 g).

Flow-through Column Exposure System

Figure 6 shows a diagram of the seawater delivery and manifold system used to expose adsorbent materials to 0.45 µm filtered ambient seawater in flow-through columns. Figure 7 is a picture of the manifold with flow-through columns attached. Seawater from a large outside storage reservoir is fed sequentially through 5 µm and then 1 µm cellulose filters and then collected in a 180 L fiberglass reservoir tank referred to as a "head tank." The seawater in the head tank is heated to the desired temperature using a 10 kW all titanium immersion heater.

Temperature-controlled (20 ± 1.5 °C) seawater is drawn from the head tank with a pump (non-metallic pump head), passes through a 0.45 µm polyethersulfone (Memtrex MP, GE Power and Water) or cellulose membrane cartridge filter and into the 24-port PVC manifold. Seawater continually recirculates through the manifold and is returned to the head tank if it does not get used for flow-through column exposure. Pressure (2-6 psi) in the manifold is controlled with a gate valve at the outlet of the manifold.

MCRL has four separate 24-port manifolds, linked to three separate head tanks, permitting testing of 96 adsorbent materials in flow-through columns simultaneously. The flow-rate of seawater passing through the columns is grossly controlled by varying the seawater delivery pressure in the manifold and then fine scale flow adjustments using a needle valve placed on the outlet of each flow-through column. A turbine flow sensor (DFS-2W, Clark Solutions) is attached to the outlet tubing to monitor and record the flow through each column. The signals from the sensors are captured by a homemade instrument package operated with National Instruments LabView software, which displays in real time the flow-rate of each column on the manifold and records integrated flow-rate measurements in increments ranging from a few seconds to several hours.

The temperature of the seawater flowing through the exposure system is monitored and recorded at the outlet of columns using an Omega model RDXL4SD handheld meter equipped with a long lead and non-metallic temperature probe. The temperature is recorded every 5-10 minutes by attaching the meter to a laptop computer using data recording and storage software provided with the instrument.

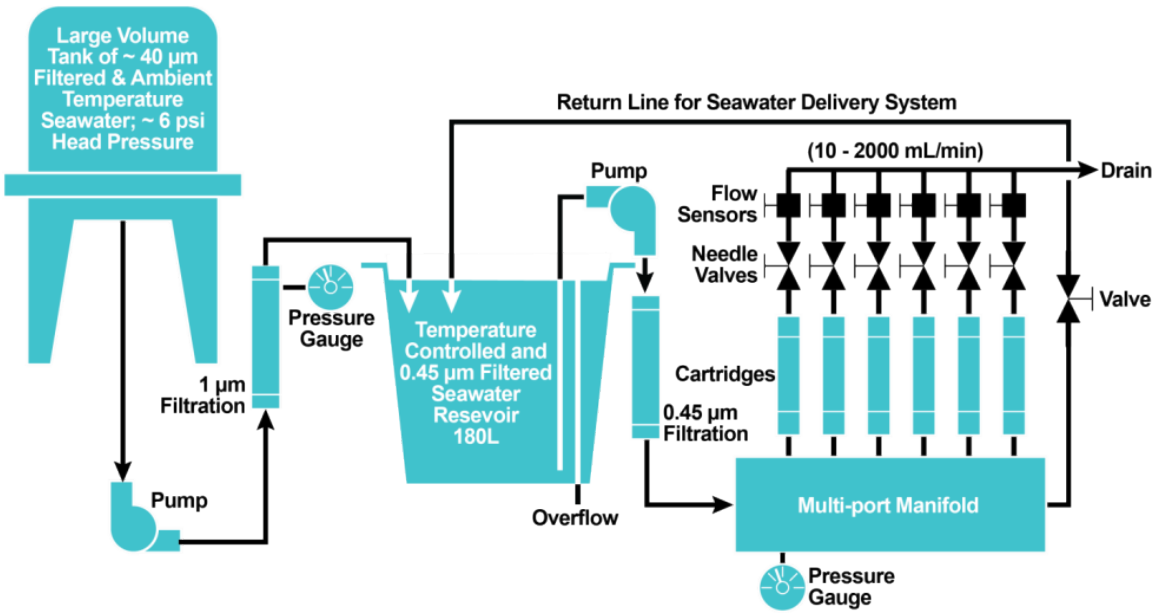

Figure 6. Layout and components of the seawater delivery and multi-port manifold system used for exposing uranium adsorbent materials in flow-through columns to filtered ambient seawater under controlled temperature and flow conditions.

Figure 7. Flow-through column exposure system.

The PNNL flow-through columns are constructed from all plastic components using commercially available materials. An example of a nominal 1-inch (2.28 cm actual) diameter column is shown in Figure 8. The column consists of a clear PVC tubing (Harvel Clear™ Rigid PVC Pipe) with threaded ends. Threaded PVC pipe fittings are used as end caps. Porous

polyethylene sheets (Bel-Art Fritware®) with pore diameter of ~ 110 µm are used to construct frits. The frits are fitted inside the end caps and serve to contain the column contents. O-rings are placed on both sides of the frit and seal the end cap to the end of the column. Five mm diameter glass beads are used as column packing material to contain the adsorbent material.

Figure 8. Nominal one-inch ID (2.28 cm actual diameter) flow-through columns packed with fiber adsorbent material.

Recirculating Flume System

The PNNL-MCSL has developed flow-through channels for conducting flume experiments under controlled temperature and flow-rate conditions. Different size pumps and flume dimensions are used to create a range in flow-rate (linear velocity). The flumes are constructed with different dimensions and recirculating pump sizes for conducting exposure tests with braided adsorbent material under controlled temperature and flow-rate (linear velocity) conditions. The target linear velocity around which the flows are varied was 2 cm/sec, which is approximately the linear velocity being used for testing with flow-through columns at PNNL. The flumes are constructed of darkened acrylic material to limit biological growth.

Shown in Figure 9 is a cross-sectional view of the flume design illustrating the recirculation system and seawater inlet. A picture of the two flumes used by this project is shown in Figure 10. Fresh seawater is fed into the flume at flow rates up to 5 L/min using the seawater manifold delivery system depicted in Figure 6. A tubing line is run from one or more of the manifold ports directly into the flume to achieve the desired seawater delivery rates. The rate of fresh seawater delivery is controlled using a needle valve mounted on one or more ports in the manifold. The height of water in the flume is controlled by the height of the stand pipe, which can be varied between approximately 7 and 11 inches (18-28 cm). Water within the flume rises until it reaches the height of the standpipe and then spills out of the flume through the standpipe. Raising or lowering the water height changes the cross sectional area of the water in the flume, which in turn is a means to control the linear velocity in the flume.

Braided adsorbents are placed into the flumes for exposure by attaching them to a short

length of ¼ inch polyethylene tubing with cable ties and inserting one end of the tubing into a small block mounted on the bottom of the flume into which a ¼ inch hole has been drilled (Figure 11). The rate at which fresh seawater is fed into the system and the internal volume of the flume controls the residence time of seawater in the system. For example, with the 6 ft. flume, the water residence time is ~20 minutes. The time to recirculate water is much faster. At a recirculation flow rate of 87 L/min, the water in the flume is recirculated once every 24 seconds.

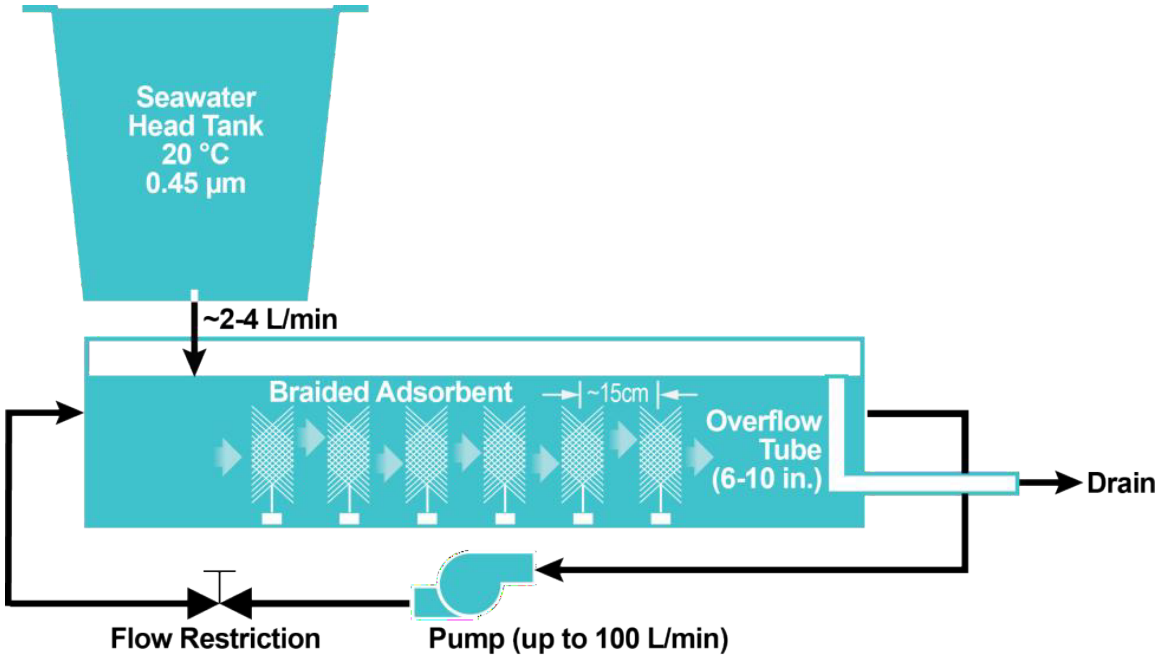

Figure 9. Side view depiction of the recirculating flume system used for exposing braided adsorbent material to filtered or unfiltered natural seawater under controlled temperature and flow-rate (linear velocity) conditions. Six braided adsorbent materials are depicted within the flume. An external pump is used to recirculate seawater in the flume. The linear velocity in the flume is controlled by a gate valve at the exit of the pump. Fresh seawater is fed into the flume using the seawater delivery system depicted in Figure 6. Seawater rises in the flume to the height of the overflow tube and then spills out at the same rate as it is introduced from the head tank.

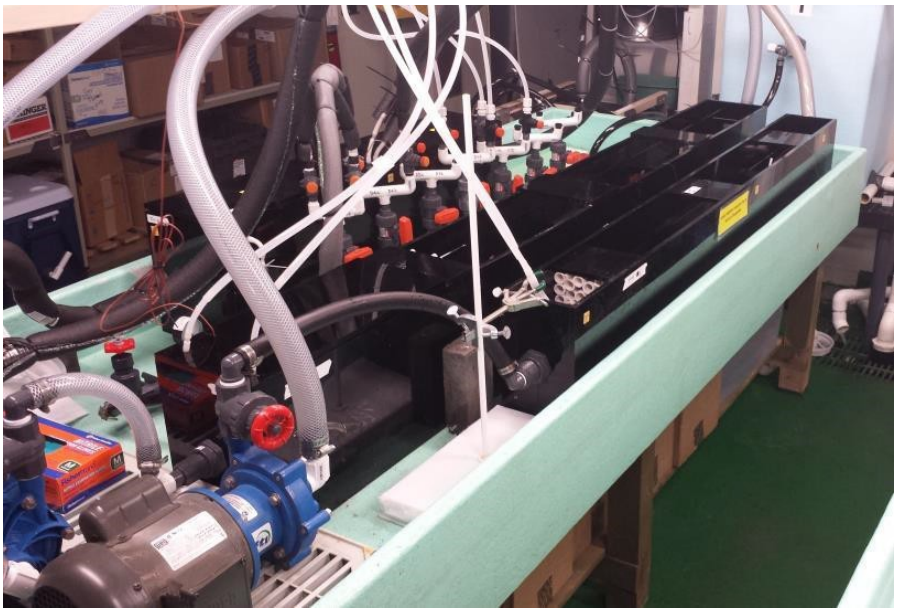

Figure 10. Recirculating flume exposure system.

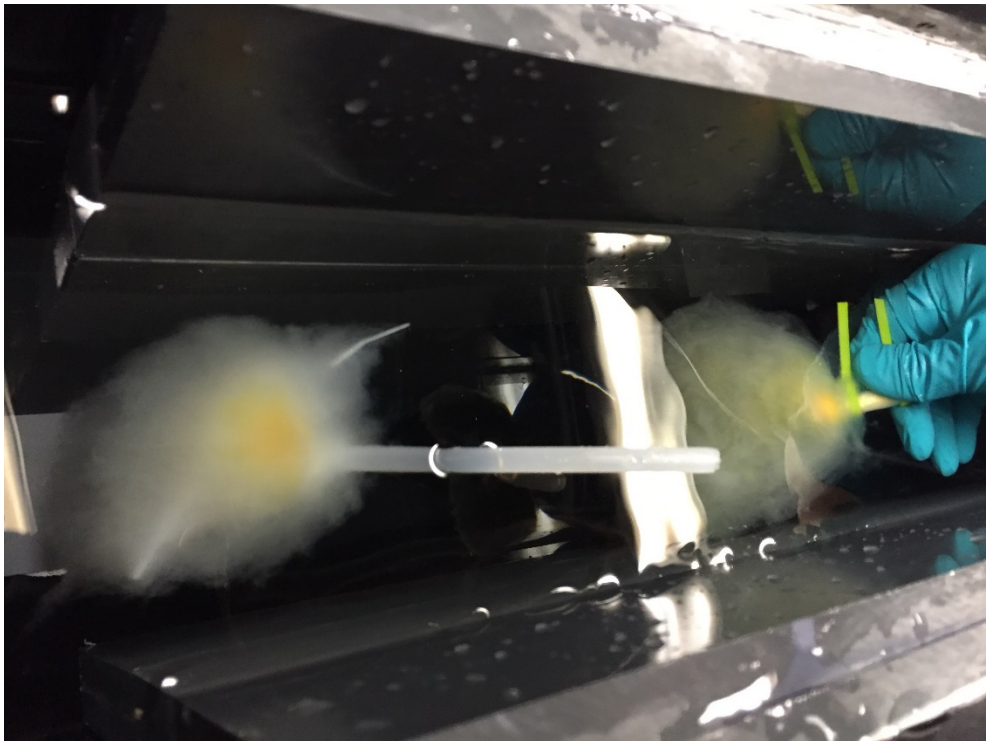

Figure 11. Adsorbent braid attached to a short length of 1/4-inch diameter polyethylene tubing. The tubing end is inserted into a PVC block attached to the bottom of the flume, fixing the braid in the flume in the desired exposure position.

Water Quality, Temperature, and Flow-rate Monitoring

Salinity and pH measurements of the seawater exposure system are obtained using hand-held probes several times a week during the exposure periods. Salinity is monitored using a YSI

model Pro30 and pH measurements are made using a portable pH meter (VWR Scientific) equipped with a temperature compensating glass electrode that is calibrated with National Institute of Standards and Technology (NIST) traceable buffers. The pH and salinity probes are calibrated weekly. High frequency (every 10 minutes) measurements of temperature in the seawater exposure systems are obtained with a thermocouple interfaced to an Omega 4 channel meter and data logger (model HH1384). Moreover, monitoring of both the seawater exposure systems and the ambient seawater is conducted with in situ YSI probes (model XLM-S in ambient seawater and a retrofitted 600 QS on the flume system) that are equipped with temperature, pH, and conductivity (salinity) probes. Both units have stand-alone data logging capability and data are recorded on an hourly basis during the exposure period to assess how conditions in the exposure system compared with ambient seawater.

IV-B. Extraction of uranium and Vanadium

Several preliminary tests were performed to optimize the uranium adsorption capacity of the fiber adsorbent. The uranium adsorption capacities of polymer fiber adsorbents produced by the chemical process described above with different NH_2OH treatment time (amidoximation time) are given in Table 1. According to our seawater tests, the fiber containing equal molar ratio of amidoxime to carboxylate groups (about 45% each, after 45 min of amidoximation time as shown in Table 1) gave the best uranium adsorption result. A small fraction of the original nitrile groups remaining in the fiber would enhance the mechanical strength of the material.[34-36] It should be noted that if all nitrile groups on the acrylic fiber surface are converted to amidoxime groups (180 min amidoximation), the fiber basically is not able to extract appreciable amount of uranium from real seawater. Comparing the FTIR spectra (Figure 12) of amidoxime-containing fibers with 45 min and with 180 min amidoximation, the $–COO^-$ band at 1595 cm^{-1} cannot be detected in the latter because it only has about 8% carboxylate groups in the fiber. This result implies that carboxylate functional groups play an important role in sequestering uranium from real seawater.

Table 1. Uranium and vanadium adsorption capacity of amidoxime-carboxylate containing polymer adsorbents derived from acrylic yarn under different amidoximation time at 70 °C.

Amidoximation Time (min)	Vanadium (g/kg)[a]	Uranium (g/kg)[a]	V/U ratio
15	0.19[b]	0.01[b]	19.0
30	3.78 ± 0.23	2.86 ± 0.14	1.32 ± 0.10
45	3.74 ± 0.21	3.61 ± 0.20	1.04 ± 0.08
60	3.03 ± 0.20	2.89 ± 0.12	1.05 ± 0.08
90	1.18 ± 0.09	0.23 ± 0.02	5.13 ± 0.59
180	0.35[b]	0.01[b]	35.0

[a]Vanadium and uranium adsorption capacity (g of metal/kg of adsorbent) after 21 days of exposure in filtered natural seawater is normalized to 35 psu. Average of 3–5 replicate seawater adsorption experiments except for 15 min and 180 min. The performance of adsorbents in real seawater was

at a temperature of 20 ± 1 °C and a flow rate of 250–300 mL min^{-1} (~2 cm s^{-1} linear velocity) by active pumping through a multi-channel flowing column system.

[b] Average of duplicate seawater adsorption experiments.

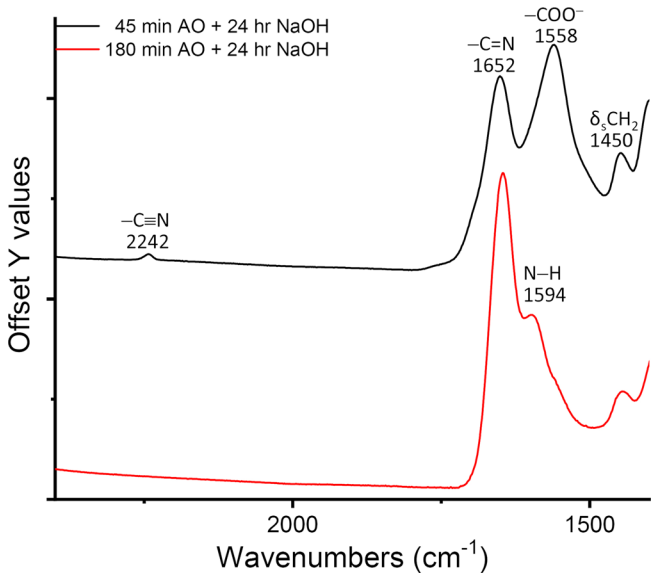

Figure 12. FTIR spectra of different amidoximation time (black, 45 min; red, 180 min) of polymer fiber adsorbents. (The spectra were normalized to the $–CH_2–$ in-plane bending or scissoring band ($\delta_s CH_2$) at 1450 cm^{-1})

The polymer fiber with this composition showed a very high uranium adsorption capacity (greater than 3.0 g uranium per kg of adsorbent after 21 days of exposure to the seawater, Figure 13a) in the flowing seawater column tests. The polymer fiber also showed a low vanadium/uranium adsorption ratio (1.04 in unit of g metal per kg fiber) relative to the adsorbents contained mainly cyclic imide-dioxime groups reported in the literature.[18-20, 29, 30, 43] Subsequent scale-up tests utilizing a circulating seawater flume system[5, 44] with braids made of ~10 grams of the fiber adsorbent confirmed the initial column test results. The uranium adsorption capacity of the braid reached 6.02 grams uranium per kg of adsorbent after 56 days of exposure in the real seawater at 20 °C (Figure 13b) and the uranium/vanadium adsorption ratio remained close to unity. Using the one-site ligand saturation model[5, 44], the estimated saturation capacity of uranium in seawater is about 7.73 grams per kg of adsorbent. The half-saturation time (15.7 days) is also shorter than those reported (>20 days) for the grafting produced amidoxime-containing fibers.[18-20, 44]

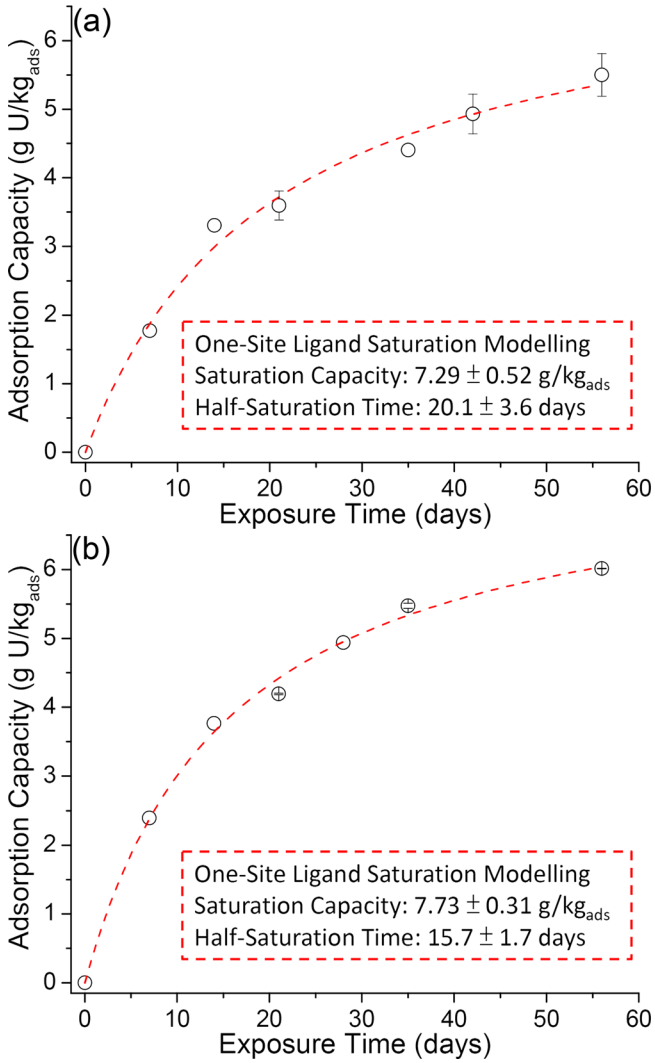

Figure 13. Time-dependent uranium adsorption results (a) fiber adsorbent in a flowing column system, (b) braided adsorbent in a circulating seawater flume system.

A comparison of the LCW adsorbent with the amidoxime-based high-surface-area adsorbents synthesized by a radiation-induced grafting method in ORNL is given in Table 2. The LCW adsorbent shows a higher uranium and lower vanadium adsorption capacity from real seawater experiments. To the best of our knowledge, this fiber adsorbent derived from acrylic fiber exhibits the lowest vanadium/uranium adsorption ratio from real seawater exposure tests among all amidoxime/carboxylate containing fibers reported in the literature.[2, 43]

Table 2 Comparison with ORNL high-surface-area adsorbent

Adsorbent	Vanadium (g/kg)[a]	Uranium (g/kg)[a]	V/U ratio
LCW	6.38	6.02	1.06
ORNL-AF1[b,18]	15.00	3.83	3.92

ORNL-AI11[b,20]	17.00	3.35	5.07
ORNL-AF1DMSO[b,19]	17.92	4.48	4.00

[a]Vanadium and uranium adsorption capacity (g of metal/kg of adsorbent) after 56 days of exposure in filtered natural seawater is normalized to 35 psu. [b]Data from references 18-20.

IV-C. Extraction of Rare Earth Elements and Other Valuable Metals

Besides U and V, the LCW fiber also adsorbs a variety of transition metals including Co, Cr, Cu, Fe, Mn, Ni, Ti, Zn in seawater (Figure 14) with good efficiencies. For example, the adsorption capacity of cobalt, a near-critical material according to DOE, is 0.27 g per kg representing a distribution coefficient (K_d) of about 10^7 between the fiber and seawater.[5] This K_d value is an order of magnitude higher than that reported for the other similar amidoxime-containing fibers.[5] Because of its high distribution coefficients for transition metals, the material may have applications in remediation and management of harmful metals in aquatic environments including contaminated waterways and industrial wastewaters.

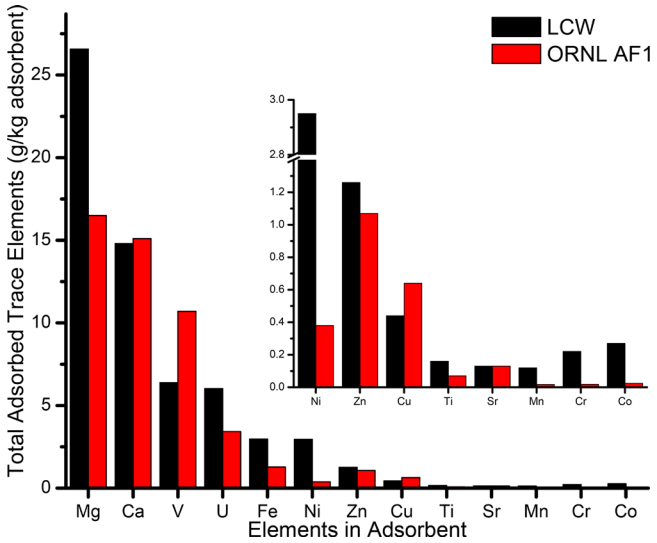

Figure 14. Some transition metals absorbed by the LCW fiber adsorbent after 56 days of exposure in the PNNL circulating seawater flume system. The data of ORNL AF1 fiber is from reference[5] for comparison. The inset is the expanded view for Ni, Zn, Cu, Ti, Sr, Mn, Cr, and Co.

Furthermore, rare earth elements (REEs) and some precious metals are also extractable from seawater by the LCW fiber although their concentrations in the fiber are low. REEs are considered critical materials according to DOE. For example, neodymium is the major component of the permanent magnet used in motors and electronic devices. The feasibility and practicality of extracting REEs from seawater deserves further study. In this report, we present our experimental observation based on the seawater uranium extraction study. The extraction of palladium by the LCW fiber in our seawater experiments is also very interesting because palladium is one of the most expensive metals today due to its indispensable usage as catalysts in many industrial processes.

As shown in Figure 15a, the concentrations of the lanthanides (from atomic number Z=57 La to Z=71 Lu) in the surface seawater (depth 3 meters) of western Pacific Ocean[45] are extremely low, in the order of parts per trillion (ng/L or ppt) or lower. Generally speaking, the light lanthanides have higher concentrations in the ocean water relative to the heavy lanthanides. Among the light lanthanides, neodymium (Nd) has a much higher concentration (about 1 ng per liter, or 1 ppt) in the ocean water relative to its neighboring elements. The adsorption pattern of the lanthanides in the Sequim Bay seawater by the LCW fiber (Figure 15b) resembles the pattern reported for the dissolved lanthanides in the Pacific Ocean. Neodymium is one of the highest extracted lanthanides found in the fiber after 56 days of exposure to the seawater. The concentration of Nd in the fiber is close to 20 mg per kg of the fiber which corresponds to a distribution coefficient (K_D = concentration of Nd in fiber/concentration of Nd in seawater) of 2×10^7.

When the K_D values of all the extracted lanthanides are plotted in the order of increasing atomic number (Figure 15c), a near linear relationship is observed favoring the heavy lanthanides over the light lanthanides. The two end members of the lanthanide series, i.e. La (Z=57) and Lu (Z=71) are slightly off the linear relationship. It is known that the radius of the trivalent lanthanide ions (Ln^{3+}) decreases as the atomic number increases in the lanthanide series, the so-called lanthanide contraction. This means the charge density of the trivalent lanthanide ions increases with the increase in Z number of the lanthanide series. Heavy trivalent lanthanides with higher charge density typically form stronger bonding in coordination with many ligands. Figure 15d suggests that chemical bonding of trivalent lanthanides with amidoxime groups occurs in the fiber and their degree of adsorption depends on the charge density of the lanthanide ions.

Palladium is extracted by the LCW fiber with a concentration of about 6 mg Pd/kg of fiber after 56 days of exposure to the Sequim Bay seawater at 20 ºC. Other precious metals extracted by the LCW fiber under the same conditions include silver (0.33 mg Ag/kg fiber) and platinum (0.11 mg Pt/kg fiber). The possibility of extracting palladium from seawater is economically interesting because palladium is more expensive than gold in the current spot market price.

According to this study, the metals extracted by LCW fiber from the Sequim Bay seawater can be roughly classified into the following groups based on their concentrations found in the fiber after 56 days of exposure:

Adsorption range per kg fiber	Elements
10–25 g	Mg, Ca
1–10 g	V, U, Fe, Ni, Zn
10^{-1}–10^{0} g	Cu, Co, Cr, Ti, Sr, Mn
10^{-2}–10^{-1} g	Y, Zr, Mo, La, Nd
10^{-3}–10^{-2} g	Ce, Pd, Lanthanides (except La, Nd, Tb, and Lu), Sc, Ga, Sn, Cd, Nb
10^{-4}–10^{-3} g	Tb, Lu, Tm, Li, Ag
10^{-5}–10^{-4} g	Pt, Bi, Te, Sb, Th, Ir

10^{-6}–10^{-5} g	Rh, Ru, Re, In, Os

It should be noted that the elements listed above is based on their detection limits of our ICP-MS analysis method. The actual concentrations of the elements found in the exposed fiber are given in the Appendix, Table A-1. The K_D values of these elements are also given in Table A-2.

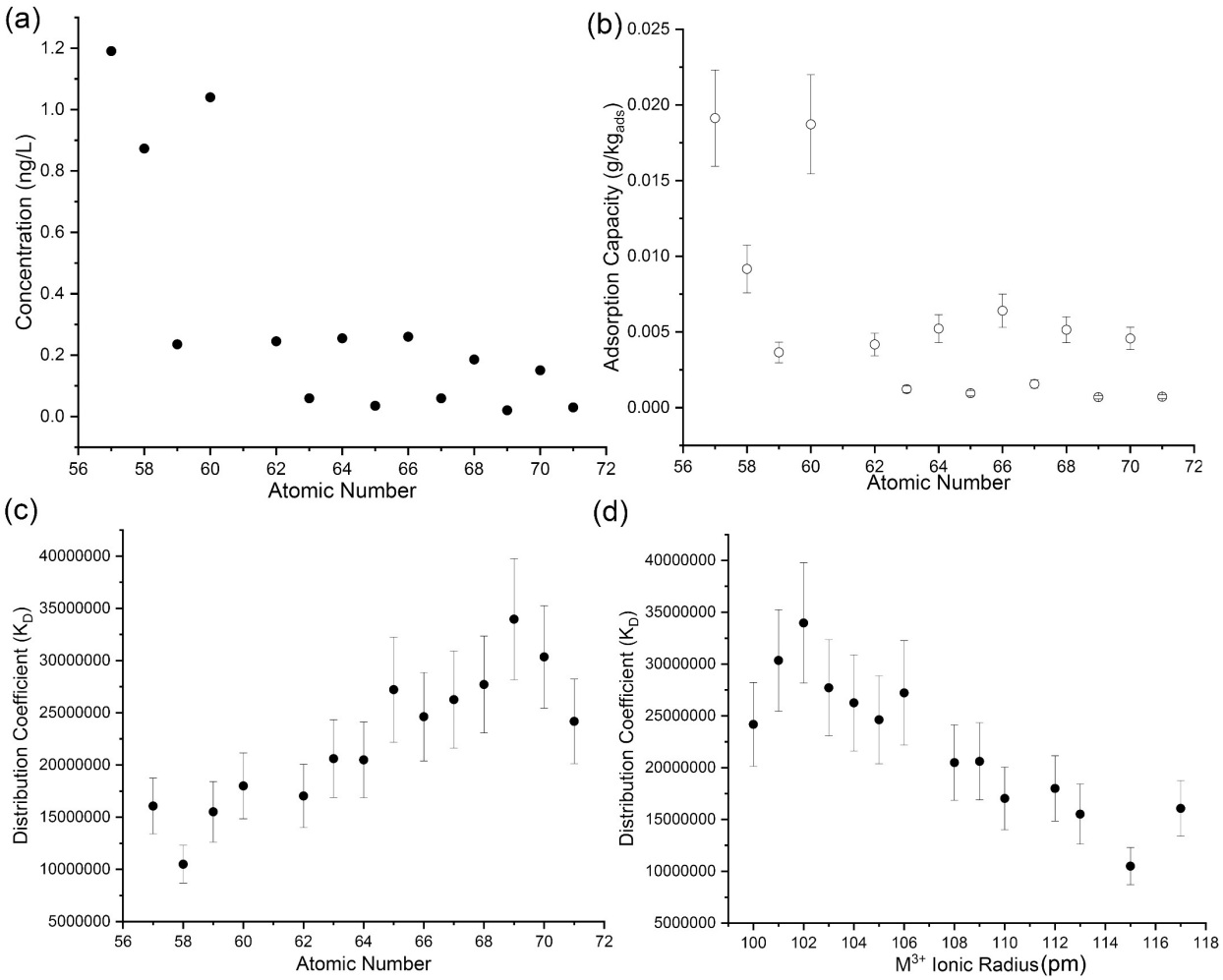

Figure 15. (a) Concentrations of lanthanides in western Pacific (depth = 3 m).[45] (b) The lanthanides adsorption capacities after 56 days of exposure to filtered natural seawater at 20 °C. Relation between the distribution coefficients (K_D) of lanthanides on the acrylic fiber-based adsorbent to (c) atomic numbers of the lanthanides and (d) ionic radii of the trivalent lanthanides (Lu^{3+} is on the left side in d).

VI-D. Elution of Uranium and Fiber Reuse

Several methods are known in the literature for elution of uranium from amidoxime and carboxylate containing fibers. Hydrochloric acid (0.5 M) was used by Japanese scientists to

remove uranium from the amidoxime/carboxylate fiber adsorbent after seawater exposure. The loss of uranium adsorption capacity using hydrochloric acid elution was assumed to be 5% per cycle in a cost analysis study published in the literature.[46, 47] A bicarbonate elution method[9] and a sodium carbonate plus hydrogen peroxide elution method[6] were also reported to work for elution of uranium from AF-1 fiber using simulated seawater in the lab. In real seawater tests, the bicarbonate and carbonate+H_2O_2 elution methods showed that the uranium adsorption capacity loss of the LCW fiber exceeded 10% in the first reuse. The reason is unknown. Hydrochloric acid elution at 0.5 M also caused about 10% of uranium adsorption capacity loss of the LCW fiber in its first reuse. However, when 0.3 M hydrochloric acid was used to elute uranium from the LCW fiber braids after seawater exposure, the results were satisfactory. About 98% of the uranium in the fiber braids could be removed by 0.3 M HCl elution at room temperature. The fiber braids after elution were washed with water and 0.5 M NaOH solution for their reuse in a circulating flume. The three fiber braids tested in this reuse experiment showed an average uranium adsorption capacity of 102% relative to the original uranium adsorption capacity.

Based on our experiments, the following procedure is recommended for elution of uranium from the seawater exposed fiber. The fiber is first treated with a dilute HCl solution at pH 2 to remove mainly calcium and magnesium from the fiber. This is followed by 0.3 M HCl elution to remove uranium. After uranium elution, the fiber is treated with 0.5 M NaOH to remove organic matters from the fiber.[48] After seawater exposure, the fiber adsorbent is dark brown to black in color. The NaOH treatment reduces the dark color of the fiber and returns the fiber to light brown color. The fiber after this treatment procedure is ready for reuse. Little is known at the present time regarding the effect of the organic matters on uranium adsorption capacity of the fiber. Organic matter adsorption probably depends on location and aquatic environment of seawater. This is one factor which deserves further research for developing fiber adsorption technology for extracting uranium from seawater.

V. Tests of Large-Scale LCW Fiber Braids for Uranium Extraction from Seawater

A circulating raceway flume system with a volume of approximately 950 liters (MicroBio Engineering, San Luis Obispo, CA), was used for evaluating the scaled-up 40-60 g masses of individual braids to extract uranium from natural seawater (Figure 16). Fresh seawater was pumped into the flume at a rate of 60 L/minute from Sequim Bay, Washington. The length of the flume system was 3.10 m and the depth was about 0.38 m. The raceway flume was fitted with a removable black plastic cover to reduce light exposure and minimize biofouling. A total of nine deployments was conducted with the total mass of adsorbent being simultaneously exposed between 0.6 and 1.0 kg each time.

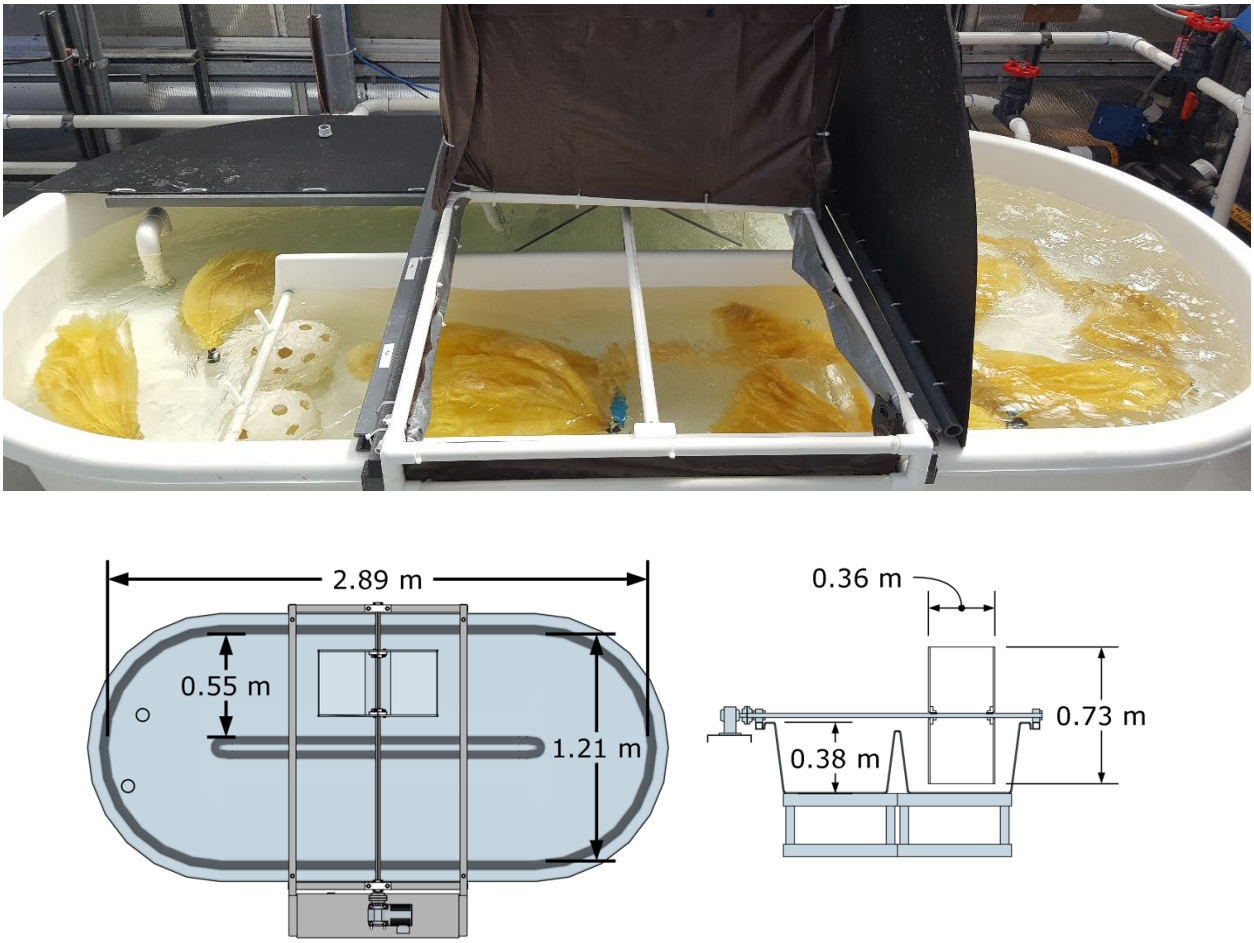

Figure 16. 950 L Raceway Flume. 9 individual LCW braids of approximately 70 g each, totaling approximately 700 g of fiber adsorbent are deployed for marine testing.

Ambient seawater was pumped from a depth of ~10 m from Sequim Bay and then filtered through an Arkal Spin Klin™ filter system (nominal pore size 40 µm) to remove large particles. The partially filtered seawater was stored in a large volume (~ 3,500 gal) reservoir tank outside the laboratory. The temperature of the seawater varied from 10-14 ºC during the LCW fiber uranium adsorption experiments. This seawater was directly fed into the raceway pond through PVC piping without additional filtration to remove finer particles. The flow rate was controlled by a transparent paddle wheel shown in Figure 16 and was determined using a handheld Acoustic Doppler Velocimeter (FlowTracker2 ADV, SonTek). Seawater salinity and pH were determined daily using a hand-held salinometer (YSI, Model 30) and a portable pH meter (Thermo Orion STAR). Seawater temperature was monitored every 10 minutes using a temperature logger equipped with a flexible, hermetic sealed, RTD sensor probe (OMEGA Engineering, Stamford, CT, USA). Seawater samples (input/output) were periodically taken to analyze uranium and other elements concentrations using ICP-MS available at PNNL-MCRL.

Adsorption experiments were conducted over a 28-day period using ambient seawater with an average temperature of ~10.8 °C in the meso-scale raceway system shown in Figure 16. Both salinity and pH remained relatively constant during the experimental period, with values of 30.5±0.3 psu and 8.07±0.03, respectively. The braided LCW adsorbent was synthesized from textile grade acrylic fibers consisting of 92% acrylonitrile and 8% methyl acrylate by weight. Adsorbents were grouped by braid size with large braids (60 g per braid) in Cage C and small braids (10 g per braid) in all other cages (Figure 17). The total adsorbent mass was about 980 g with 800 g of small braids divided evenly between the eight cages containing small braids and 180 g of large braids in Cage C. Adsorbent snips were collected weekly from the tips of the adsorbent braids in Cages B and C using titanium-coated scissors and analyzed to determine the adsorbed mass of uranium and other metals. Snipped samples were first washed with deionized water and then dried at 80 °C using a heating block overnight.

Dried adsorbent snips were then digested in 15 mL of Fisher Scientific Optima® grade 50% aqua regia acid solution consisting of a 3:1 hydrochloric-nitric acid mixture for 3 hours at 85°C. Analysis of the digestate was carried out using a PerkinElmer 7300 inductively coupled plasma optical emission spectrometer (ICP-OES) and quantified based on standard calibration curves. The aqueous concentration of uranium and vanadium was determined using inductively coupled plasma mass spectroscopy with the on-line pre-concentration method.[49] This method was carried out using an Elemental Scientific seaFAST S2™ equipped with a seaFAST PFA chelation column packed with ethylenediaminetriacetic/iminodiacetic acid ion exchange resin. Analytes were eluted off the column using 10% HNO_3 and then nebulized for analysis by a Thermo Scientific ICap Q inductively coupled plasma mass spectrometer (ICP-MS).

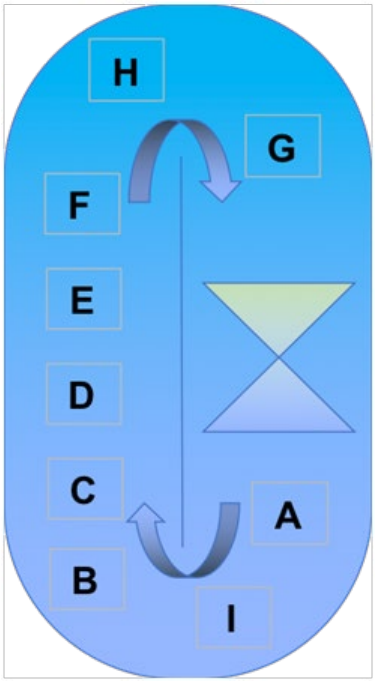

Figure 17. Schematic of the cages containing adsorbent braids in the raceway where Cage C contains three large braids (60g per braid) while all other cages contain ten small braids (10g per braid).

The adsorption of uranium and other metals on amidoxime based fibers is primarily governed through adsorbent-adsorbate reaction kinetics and the mechanisms of mass transfer including inter-particle, inter-phase, and intra-particle mass transfer.[50] At the experimental linear velocity of about 8 cm/s, however, the mass-transfer limitations in the flume are removed and as such do not need to be considered.[51] To account for adsorption, all adsorbent-adsorbate reactions are assumed to proceed as reversible Langmuir type reactions (Equation 1) where C is the adsorbate concentration in the bulk phase, q is the adsorption capacity represented as mass adsorbed per mass of adsorbent, and L is the capacity still available for adsorption. This available capacity L is in turn a function (Equation 2) of the theoretical maximum capacity ($q_{\max}$) and q. Equations 1 and 2 can be combined to derive a kinetic expression for adsorption (Equation 3) with forward and reverse reaction rate constants of k_f and k_r, respectively. For the bulk phase, the system is treated as a series of perfectly mixed reactors defined by Equation 4. In this equation, V is the reactor volume, M_a is adsorbent mass, C_j is the concentration of the jth element in the reactor, Q_i is the ith incoming flowrate, C_{ij} is the ith influent concentration of the jth element, Q_o the oth outgoing flow, and q_j is the adsorbent mass of the jth element. A series of ten perfectly mixed reactors corresponding to the nine adsorbent cages shown in Figure 17 and the section of the raceway where concentration is monitored is considered when modeling is performed. The forward and reverse reaction rates and maximum adsorption capacity is summarized in Table 7.

$$C + L \Leftrightarrow q \tag{1}$$

$$L = q_{\max} - q \tag{2}$$

$$\frac{\partial q}{\partial t} = k_f C q_{\max} - (k_f C + k_r) q \tag{3}$$

$$V \frac{\partial C_j}{\partial t} = \sum Q_i C_{ij} - \sum Q_o C_j - M_a \frac{\partial q_j}{\partial t} \tag{4}$$

Table 7. Forward (k_f) and reverse (k_r) reaction rate constants for uranium (U), vanadium (V), and zinc (Zn) and adsorbent max capacity (mol/kg adsorbent) for small and large braids.

		Small Braids	Large Braids
$q_{\max}$ (mol/kg)		1.47	1.47
	U	0.75	0.544
k_f (m^3/mol/hr)	V	2.75	2.0
	Zn	1.25	0.906

	U	0.00107	0.00107
k_r (1/hr)	V	0.00275	0.00275
	Zn	0.00625	0.00625

After an exposure period of 28 days, the salinity normalized uranium recovery rate for small LCW braids in Cage B was 1.43 mg/g adsorbent while the large braids in Cage C had a uranium capacity of 1.17 mg/g adsorbent (Table 5). The disparity in uranium recovery between the small and large LCW braids can likely be attributed to complications arising from material scale-up. At first glance, these recovery rates may appear lower that the rates previously observed with a similar acrylic adsorbent material, which attained a uranium recovery rate of approximately 4.4 mg/g adsorbent over 28 days filtered seawater exposure.[52] These experiments, however, were performed at an average temperature of 20°C, compared to the 10.8°C maintained on average for this study, and with finely filtered seawater (0.45-µm nominal pore size). The effect of temperature on uranium uptake for LCW adsorbents has not been studied, however, temperature dependent adsorption in other amidoxime based materials developed at Oak Ridge National Laboratory (ORNL) has been analyzed.[8, 53] In the case of ORNL's AF1 series adsorbent using 0.45 µm filtered Sequim Bay seawater, the salinity normalized 21-day recovery rate for small braids dropped from 2.5 mg uranium/g adsorbent at 20 °C to 0.93 mg uranium/g adsorbent at 8 °C.[8] This is a result of uranium adsorption to amodixime-based adsorbents being highly endothermic (apparent enthalpy ~58 kJ/mol).[8, 53] Therefore, the reduced uranium adsorption capacity in the present study can be attributed to this temperature effect.

The filtration level may also affect adsorption through adsorbent biofouling. Coarse filters, such as the 40-µm pore size filter used in this study, allow microorganisms to infiltrate the system and colonize the adsorbent braids. This leads to a reduction in the materials adsorption capacity, though it also offers a more realistic idea of the adsorbent's capacity when deployed in the open ocean. Capacity loss from biofouling can be as high as 30% under worst case conditions (fully exposed to light) at 20 °C.[54] For the experiment in the present study, it is highly unlikely that the adsorbents would experience worst case capacity losses since the raceway was covered leaving the braids in complete darkness for most of the experiment. This inhibits the growth of photosynthetic microbes which play an important role in microbial colonization of the adsorbent braids. Park and coworkers previously showed that in a dark flume feed with coarsely filtered seawater (150-µm pore size) adsorbents accumulated 75% less microbial mass than adsorbents exposed to light after 42 days at 20 °C.[54] At this significantly reduced biomass, the disparity between the capacity of the adsorbent in the coarsely filtered dark flume and the finely filtered control flume was negligible. Additionally, the lower temperature of the present experiment is likely to inhibit microbial growth even further. Thus, while some biomass accumulation is observed on the adsorbent, it is unlikely to have a significant impact on the adsorption capacity.

Table 5. Concentration in feed seawater and salinity normalized 28-day adsorption capacities on small braids in Cage B (LCW-B) and the large LCW braids in Cage C (LCW-C) for uranium, vanadium, iron, copper, and zinc at 10.8 ºC.

	Concentration in feed seawater	LCW-B		LCW-C	
	nM	mg/g	µmol/g	mg/g	µmol/g
Uranium	12.8	1.43	6.01	1.17	4.92
Vanadium	36.2	1.90	37.25	1.26	24.71
Iron	545.3	1.86	33.21	1.71	30.54
Zinc	22.1	0.44	6.77	0.31	4.77
Copper	7.5	0.03	0.47	0.02	0.31

Trace elements including iron, copper, zinc, and vanadium are also adsorbed and are competitors to uranium for amidoxime adsorption sites.[5, 55] Vanadium, in particular, binds very favorably to amidoxime and is present at a slightly higher concentration in Sequim Bay than the 30 nM global average concentration.[56] For this study, the mass of vanadium adsorbed over the 28 day exposure period was 1.9 mg/g adsorbent for small LCW braids in Cage B and 1.26 mg/g adsorbent for large LCW braids in Cage C. A greater mass of vanadium was reported on a similar acrylic adsorbents in our previous test, reaching about 4.0 mg/g adsorbent after 28 days at 20 ºC.[24] This disparity could be explained by a few different factors though further analysis of the LCW adsorbent will be needed to determine the precise mechanism. Past analysis of ORNL's AF1 and AI8 amidoxime adsorbents has shown that the adsorption of vanadium is not significantly impacted by temperature.[8] If this behavior can be extended to the LCW adsorbents, then this would suggest significant refinement of the present LCW materials over earlier formulations.

Compared to the materials developed at ORNL, vanadium adsorption on the LCW adsorbent is quite low for the same vanadium aqueous concentration. At 8 ºC, the adsorbed mass of vanadium after 28 days exposure to Sequim Bay seawater for ORNL's AF1 and AI8 adsorbents formulated in small braids was approximately 8.5 mg/g adsorbent and 8.0 mg/g adsorbent, respectively.[8] This makes the V/U ratio (w/w) of ORNL adsorbents ~8 at 8ºC; while the V/U ratios of LCW adsorbents tested in the present study are only ~1.2 for braids of a similar size. Indeed, one unique feature of LCW adsorbents is their much lower vanadium adsorption.[42] Although some recent studies[8, 54] have indicated that uranium and vanadium do not directly compete for the same adsorption sites, limiting vanadium uptake can be still advantageous. This is due to vanadium's high binding affinity with certain amidoxime sites which requires harsh acidic treatment that damages the adsorbent to effectively strip the vanadium.[31] Thus by substantially reducing the adsorption of vanadium, it is possible to significantly increase the reusability of the adsorbent, which is critical to the economic viability of uranium recovery from seawater.[4]

Of the remaining trace elements, iron is the most important with an amidoxime binding strength and adsorption rate similar to those of uranium.[57, 58] The 28-day adsorption capacity was 1.90 mg/g adsorbent for the Cage B small braids and 1.71 mg/g adsorbent for the Cage C large braids. This adsorption rate is roughly on par with the adsorption of vanadium and several times greater than that of uranium, in terms of molar adsorption, while having a total aqueous concentration (feed seawater) about 15 times higher than the concentration of vanadium. Iron complexation in seawater is, however, very complex with a large proportion of aqueous iron in both organic and inorganic forms that are unavailable for adsorption on amidoxime adsorption sites.[55] Thus, based solely on the total aqueous concentration, it is difficult to accurately assess the performance of the LCW materials with respect to their selectivity of iron over uranium. Adsorption of copper on both samples is effectively negligible with only about 30 μg adsorbed per g adsorbent on the small braids in Cage B. Lastly, while the molar adsorption of zinc is comparable to uranium, the binding affinity of the amidoxime ligands for zinc is not precisely known, though it appears to be weak.[55, 59]

The adsorption capacity for uranium, vanadium, and zinc on both the Cage B small braids (Figure 18) and Cage C large braids (Figure 19), and the aqueous concentration of uranium and vanadium (Figure 20) over the experimental period were simulated using the modeling methodology previously described. Estimates of the adsorption capacity were made by adjusting the forward and reverse rate constants for both samples. Initially, this approach under-predicted the aqueous concentration in the flume, thus a correction was applied reducing the total simulated mass by 15%. Most of this correction can be attributed to the methyl acrylate comonomer which makes up 8% of the braids' total mass and does not participate in adsorption. Additionally, when the braids are attached to the Cage frame the base of the braid is tightly bound, significantly constricting the flow of seawater through that region of the braid. Thus, the adsorbent mass located in the constricted area is, aside from material on the surface of the braid, unavailable for adsorption.

Biofouling was assumed to have no impact on the capacity of the adsorbent. With this rate information, it is possible to simulate the adsorbent's 56-day and saturated adsorption capacities which are summarized for the Cage B small braids (Table 6) and Cage C large braids (Table 7). The salinity normalized adsorption capacities on the Cage B small braids for uranium, vanadium, and zinc are 2.45 mg, 2.63 mg, and 0.48 mg per g adsorbent at 10.8 ^{o}C, respectively. For the large braids in Cage C, the salinity normalized capacities were 1.78 mg uranium, 1.92 mg vanadium, and 0.35 mg zinc per g adsorbent at 10.8 ^{o}C. Based on the work of Kuo and coworkers,[8] the uranium adsorption capacity of ORNL's AF1 and AI8 adsorbents can be simulated at our experimental temperature in Sequim Bay seawater. This results in a salinity normalized uranium adsorption capacity of 1.68 mg/g adsorbent for AF1 and 1.36 mg/g adsorbent for AI8 at 10.8 ^{o}C after 56 days. With respect to vanadium, at the lowest temperature examined by Kuo and coworkers (8^{o}C), the salinity normalized vanadium adsorption capacities after 56 days for AF1 and AI8 in Sequim Bay seawater were 13 mg/g adsorbent and 14 mg/g adsorbent, respectively. Thus, at reduced temperatures, the small LCW braids significantly outperform both the AF1 and

AI8 adsorbent small braids with respect to uranium capture, while also adsorbing substantially less vanadium.

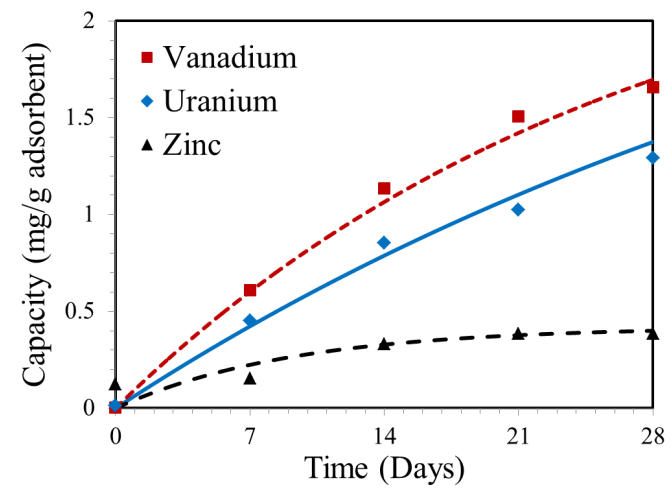

Figure 18. Simulated (lines) and experimental adsorption capacities (mg adsorbate/g adsorbent) for vanadium, uranium, and zinc over the 28-day exposure period for Cage B small braids in raceway.

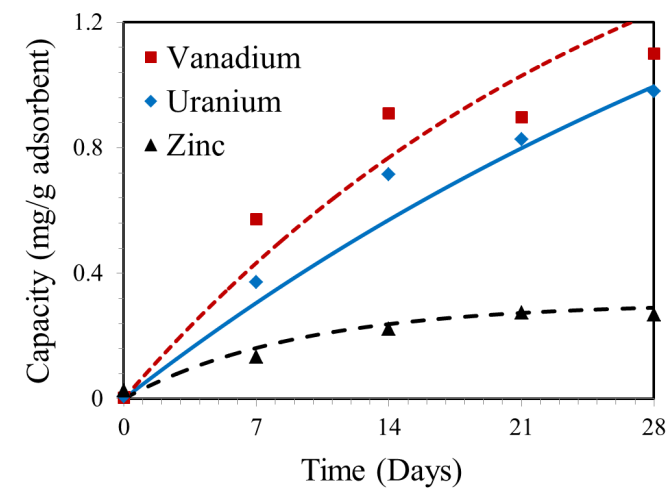

Figure 19. Simulated (solid lines) and experimental adsorption capacities (mg adsorbate/g adsorbent) for vanadium, uranium, and zinc over the 28-day exposure period for Cage C large braids in raceway.

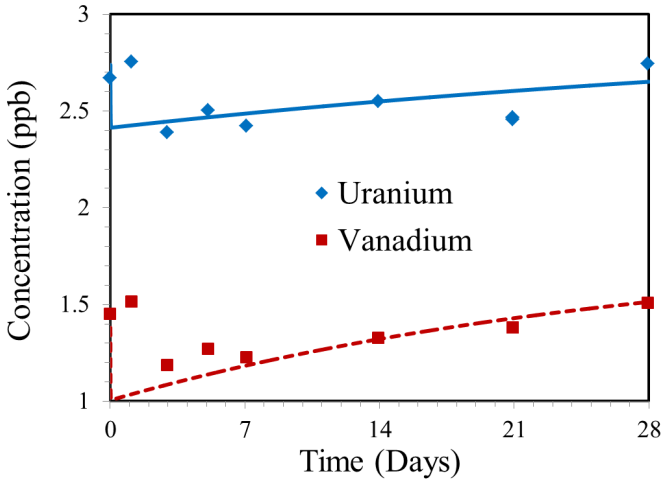

Figure 20. Measured and simulated (solid lines) aqueous concentrations (ppb) for uranium and vanadium in raceway over the 28-day exposure period.

To estimate the performance of the LCW braids at higher temperatures, at least one additional reference point is needed. Thus, it was assumed that at 20 °C, adsorption on the LCW braids under ideal conditions is comparable to the similar acrylic adsorbent previously studied.[52] From these data, the forward and reverse rate constants for adsorption of vanadium, uranium, and zinc can be estimated and used in the adsorption model. For the purpose of this simulation, vanadium adsorption was assumed to increase with increasing temperature. This is not necessarily the case though, as noted previously, it is a strong possibility and cannot be ruled out based on our current knowledge of the material. With this kinetic information, the salinity normalized adsorption capacities in the raceway can be estimated at 20 °C. The simulated 56-day capacities for uranium and vanadium at 20 °C on the Cage B small braids are 4.68 mg and 4.44 mg/g adsorbent, respectively (Table 6).

Table 6. Simulated 56-day, salinity normalized raceway adsorption capacity (mg/g) and saturated adsorption capacity (mg/g) for vanadium, uranium, and zinc on the small braids.

	56-day Capacity (mg/g adsorbent)			Saturation Capacity (mg/g adsorbent)		
	10.8°C	20°C	31°C	10.8°C	20°C	31°C
Vanadium	2.63	4.44	6.91	3.00	5.97	12.32
Uranium	2.45	4.68	7.77	3.49	5.53	9.07
Zinc	0.48	0.75	1.23	0.48	0.75	1.23

Once again, the LCW adsorbent outperforms both the AF1 and AI8 adsorbents for samples of similar braid size though to a lesser degree than at 10.8 °C, adsorbing only 20% more uranium than AF1 at 20 °C compared to 45% more at 10.8 °C. Additionally, the adsorption of vanadium is

still substantially lower than the 13 mg/g adsorbent on AF1 small braids and 16 mg/g adsorbent on observed AI8 small braids.[8]

Table 7. Simulated 56-day, salinitiy normalized raceway adsorption capacity (mg/g) and saturated adsorption capacity (mg/g) for vanadium, uranium, and zinc on large braids.

	56-day Capacity (mg/g adsorbent)			Saturation Capacity (mg/g adsorbent)		
	10.8°C	20°C	31°C	10.8°C	20°C	31°C
Vanadium	1.92	3.24	5.05	2.20	4.08	9.30
Uranium	1.78	3.39	5.65	2.57	4.03	5.43
Zinc	0.35	0.54	0.90	0.35	0.55	0.89

On the larger braids (Table 7), 56-day salinity normalized adsorption is simulated to be about 29% lower than on the small braids for both uranium and vanadium. This estimate was obtained by assuming that the impact of adsorbent scale up remains constant at all temperatures. With experimentally determined rate information for 10.8 °C and an estimate of the rate constants at 20 °C, a rough estimate of the forward and reverse rate constants can be obtained at other temperatures using the Arrhenius equation and applied to the adsorption model. Thus, the simulated 56-day 31 °C uranium capacity is 7.77 mg/g adsorbent with a 56-day 31 °C vanadium capacity of 6.91 mg/g adsorbent for the Cage B small braids (Table 6). At 31°C, and for adsorbent braids of similar size, the AF1 adsorbent slightly outperforms the LCW material with a 56-day uranium adsorption capacity of 7.8 mg/g adsorbent, though the adsorption on AI8 is lower at 6.5 mg/g adsorbent. Nevertheless, vanadium adsorption on the AF1 adsorbent is ~3.4 times higher than is simulated to adsorb on LCW small braids at 31 °C. Thus, the LCW materials are expected to outperform or match adsorption of ORNL's AF1 and AI8 adsorbents of similar size at all relevant temperatures, while also having a substantially reduced affinity for vanadium. The LCW adsorbents adsorb significantly less vanadium, thus reducing the need for harsh elution of the adsorbent and increasing its reusability. Considering LCW's potential for lower cost production and conditioning, they may offer an avenue to notably reduce the cost of uranium recovery from seawater.

VI. Production of Yellowcake

Production of yellowcake from seawater using the fiber adsorbent involves several steps including uranium adsorption, elution, concentration, and precipitation. Adsorption of uranium from seawater using LCW fiber has been extensively discussed in the previous sections. Several elution methods for removing adsorbed uranium from the fiber are known in the literature including acid elution, bicarbonate elution, sodium carbonate-hydrogen peroxide elution.[6, 9, 31, 46] Acid elution of uranium from the amidoxime/carboxylate fiber is a traditional method used by many previous uranium-from-seawater studies. Typically, hydrochloric acid is used to elute the adsorbed uranium from the fiber. At 0.01 M, HCl is not able to elute uranium from LCW fiber.

Elution of uranium from the fiber becomes appreciable above 0.1 M HCl. For example, using 0.3 M HCl about 98% of adsorbed uranium can be eluted from the fiber.

Acid elution can be tied to the known process of extracting uranium from acid solution into organic solvents with tri-n-butyl phosphate (TBP) to achieve uranium separation and concentration. For example, in the PUREX process uranium dissolved in 3M nitric acid is extracted into kerosene with TBP forming a neutral uranyl-nitrate-TBP complex $UO_2(NO_3)_2$•2TBP in the organic phase. Back-extraction of uranium from the organic phase can be achieved using 1 M ammonium carbonate $(NH_4)_2CO_3$ solution. After back-extraction, by heating the ammonium carbonate solution to boiling and under reflux condition, precipitation of ammonium uranyl carbonate $(NH_4)_4[UO_2(CO_3)_3]$ yellowcake occurs. In a fluidized bed furnace, ammonium uranyl carbonate is decomposed to UO_3 and reduced to UO_2 using an atmosphere of H_2 and H_2O vapor.[60] In addition, U_3O_8 can be obtained through the calcination of ammonium uranyl carbonate.[60] U_3O_8 can also be used as nuclear fuel for research reactors. For demonstration purpose, we simplified the elution-extraction process using 3 M nitric acid for elution and 30% TBP in hexane as the organic solvent for extraction. Before uranium elution, the fiber is treated with 0.01 M HCl to remove calcium, magnesium and other soluble elements. The process of uranium elution from the fiber and production of yellowcake is illustrated in the flow diagram shown in Figure 21.

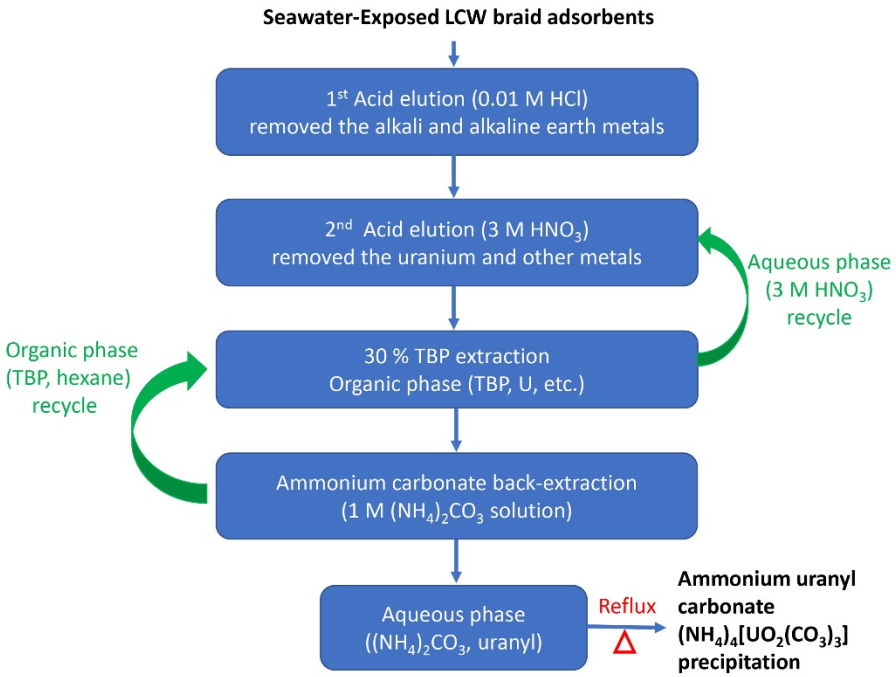

Figure 21. Flow chart of uranium elution and production of yellowcake.

The uranium concentration in the acid solution was determined spectrophotometrically using an Arsenazo III method as shown in Figure 22a. The uranyl-arsenazo complex has an absorption peak at 656 nm. After the solvent extraction with TBP in hexane, the concentration of

uranium in the acid solution decreases with increasing TBP in hexane as shown Figure 22a indicating migration of uranyl from the aqueous phase into the organic phase. Above 30% TBP in hexane (v/v), the extraction of uranium from the aqueous solution reaches a maximum. The UV-Vis spectrum of the organic phase shows multiple absorption peaks corresponding to those observed with the uranyl-nitrate-TBP complex [$UO_2(NO_3)_2$•2TBP] shown in Figure 22b.

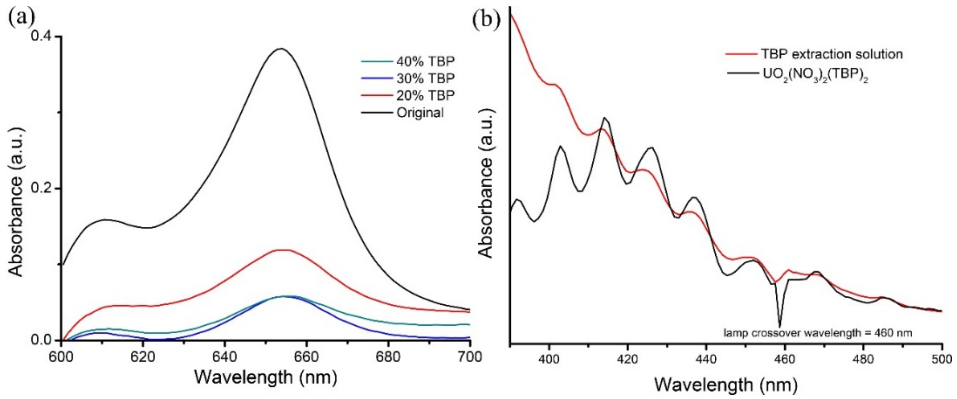

Figure 22. (a) Absorbance spectra of the Arsenazo III- Uranium complex; (b) Absorbance spectra of the uranyl nitrate–TBP complex ($UO_2(NO_3)_2$•2TBP).

Uranium in the organic phase can be back-extracted into 1 M $(NH_4)_2CO_3$ at room temperature. Figure 23a shows the yellow ammonium carbonate (1 M) solution after back-extraction indicting the presence of uranium in the carbonate solution. Figure 23b shows the formation of ammonium uranyl carbonate precipitation after heating the solution to boiling and under reflux for 1 hour. The yellowcake powder was collected by filtration.

About 4 grams of dry yellowcake (Figure 23c) were produced from Sequim Bay seawater in 2018 using a raceway recirculating flume system at PNNL's Marine and Coastal Research Laboratory.

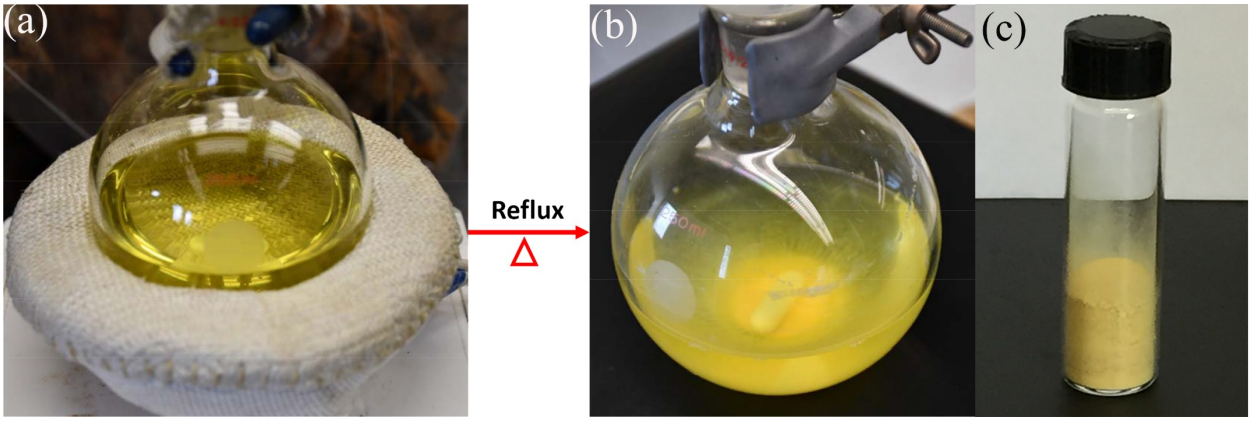

Figure 23. (a) Eluted uranium in ammonium carbonate solution; (b) Precipitation formation of ammonium uranyl carbonate after reflux; (c) About 4 grams of dry yellowcake $(NH_4)_4[UO_2(CO_3)_3]$

VII. Direct Warm Seawater Deployment

Testing of LCW fiber for adsorption of uranium from seawater was mainly done at PNNL's Marine and Coastal Research Laboratory (MCRL) using circulating flume systems utilizing Sequim Bay seawater which has an average temperature of 12 ºC. Direct deployment of the fiber for adsorption of uranium in warm marine environment was performed in Galveston, Texas. The choice of Galveston, Texas is based on the fact that the average temperature of the seawater in Galveston is around 28 ºC which is about 16 degrees (ºC) higher than the seawater at Sequim Bay, Washington. In addition, Dr. Gary Gill our collaborator at PNNL knows the Oceanography Department of the Texas A&M University Galveston (TAMUG) well. Based on his arrangements, a contract between LCW and TAMUG was signed in the summer of 2019. Professor Peter Santschi of TAMUG supervised the performance of the warm seawater uranium adsorption experiments using the LCW long fibers prepared in our Idaho laboratory. The purposes of the warm seawater study include: (1) obtain adsorbent performance data from raw seawater exposure (field test) and (2) assess the performance of LCW adsorbents in warm and cold seawater conditions.

Drs. Gary Gill and Li-Jung Kuo from MCRL designed the experiments and instructed/oversaw the deployments/sample collections in the TX field site. The selected site is located at the East Pier near TAMUG campus. This site is in a walking distance from the building of Department of Marine Sciences but is not easily accessible to general publics. The location of the sampling site is shown in Figure 24.

Figure 24. Deployment site for the field test in Galveston, TX (images were obtained from Google Maps).

Based on the bathymetry of sampling site, we concluded that customized davits with extended arms are needed for the deployment of LCW braids. Three customized davits were built.

One davit was used for sensor deployment; other two davits were used for braids in 2 and 4 meters water depth, respectively. Figures 25 shows the customized davits with concrete bases in the deployment site. Five two-meter and three four-meter 28d deployments were completed representative of a range of seasonal conditions. Adsorbents were subsampled at 7, 14, 21, and 28d timepoints following clean-hands/dirty-hands techniques (EPA 1996). Duplicate or triplicate samples were collected frequently to report amidoximation and biofouling induced variability.

Figure 25. Three customized davits were installed on the pier near the deployment site.

Water quality parameters (temperature, salinity, and pH) in the Galveston Channel were spot checked daily using a portable meter. Salinities were measured daily using a YSI model Pro30 instrument (Yellow Springs, OH, USA). Temperatures were logged every 5 minutes by Omega Engineering (Norwalk, CT, USA) RDXL4SDs equipped with nonmetallic probes and verified daily by the YSI model Pro30, which in-turn was verified quarterly by a National Institute of Standards and Technology traceable thermometer. pH was recorded periodically, in laboratory and field studies, using an Orion meter (Waltham, MA. USA). Additionally, dissolved organic carbon was measured in both laboratory and field systems periodically, as an ancillary parameter, using a Shimadzu TOC-L (Kyoto, Japan) equipped with a saltwater column. Summary seawater parameters for all studies are provided in Table 3. For continuous surveillance, a Sea-Bird Scientific (Bellevue, WA, USA) MicroCAT CTD was continuously moored at 4m depth to log temperature and salinity at 5-minute intervals. Additionally, photosynthetically active radiation (PAR) was monitored during select periods, using LI-COR (Lincoln, NE, USA) LI-193SA spherical underwater quantum sensors, as an approximation of biofouling rate potential.

Table3. Average water quality parameters for each deployment.

Adsorbent ID	Conditions	Location	Avg. Temp. (°C)	Avg Sal. (PSU)	Avg. pH	Avg. DOC (mg L^{-1})
3588-29	TAMUG-1	Galveston Channel*	29.0	20.1	6.75	3.00
3588-29	TAMUG-2	Galveston Channel†	18.1	21.5	7.18	2.45
3588-29	TAMUG-3	Galveston Channel‡	20.1	20.1	7.78	2.97
3588-29	TAMUG-4	Galveston Channel§	28.8	23.6	7.46	4.21
3588-29	TAMUG-5	Galveston Channel‖	30.4	27.8	7.72	2.98

*, §, ‖: calculated from 2m data points; †, ‡: calculated from 4m CTD points

Average ambient water quality during TAMUG's third field test (Figure 26) was similar to the second deployment period. PAR (Figure 27) in the euphotic zone was highest during this deployment period, exceeding 1000 µmol s^{-1} m^{-2} at solar noon. This increase in PAR during winter months indicates that a drop in algae concentrations could explain the U adsorption results given in Figure 27, where uptake in the 2 m layer agrees well with predicted performance. Uptake in the 4 m layer still fell significantly below the predicted curve due to a coating of suspended sediments, resulting from its placement near the benthic boundary layer. Deployments at 4 m were discontinued after TAMUG's third test. The 2 m deployment during this test period reflects optimal convergence of ambient conditions for this highly variable site and highlights the necessity to select stations that are not highly affected by proximity to land-based influences.

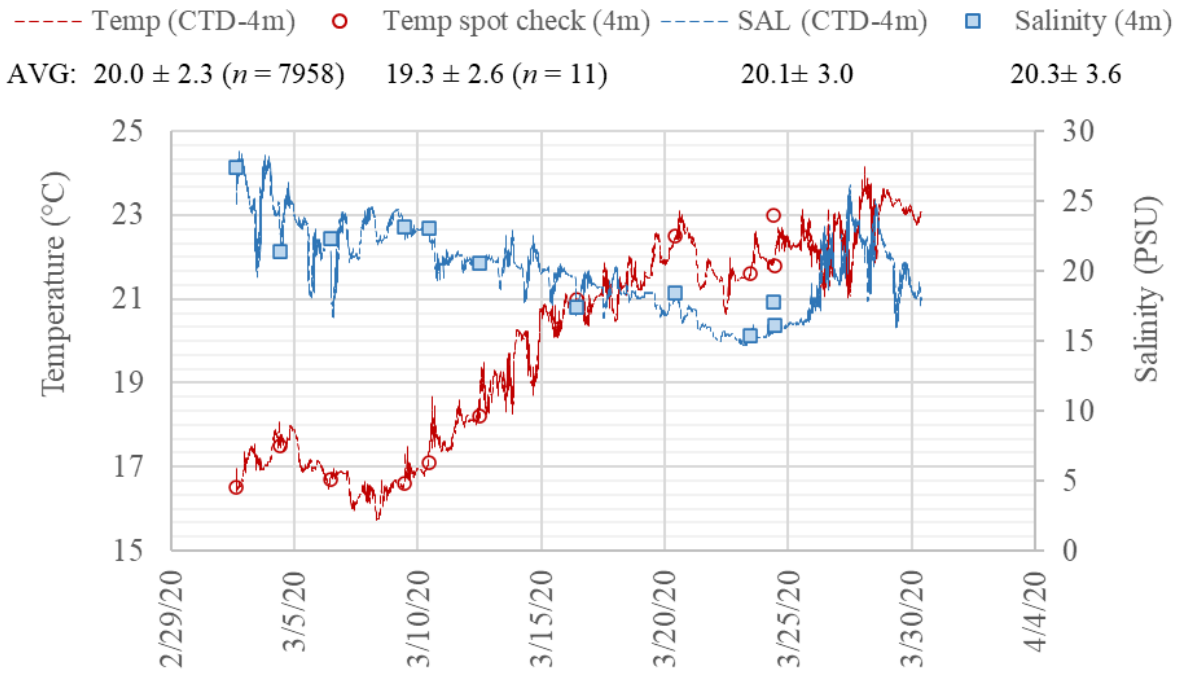

Figure 26. Galveston Channel temperature and salinity measurements, collected by combination of CTD and hand-held instrumentation, over the period from 03/02/20 – 03/30/20.

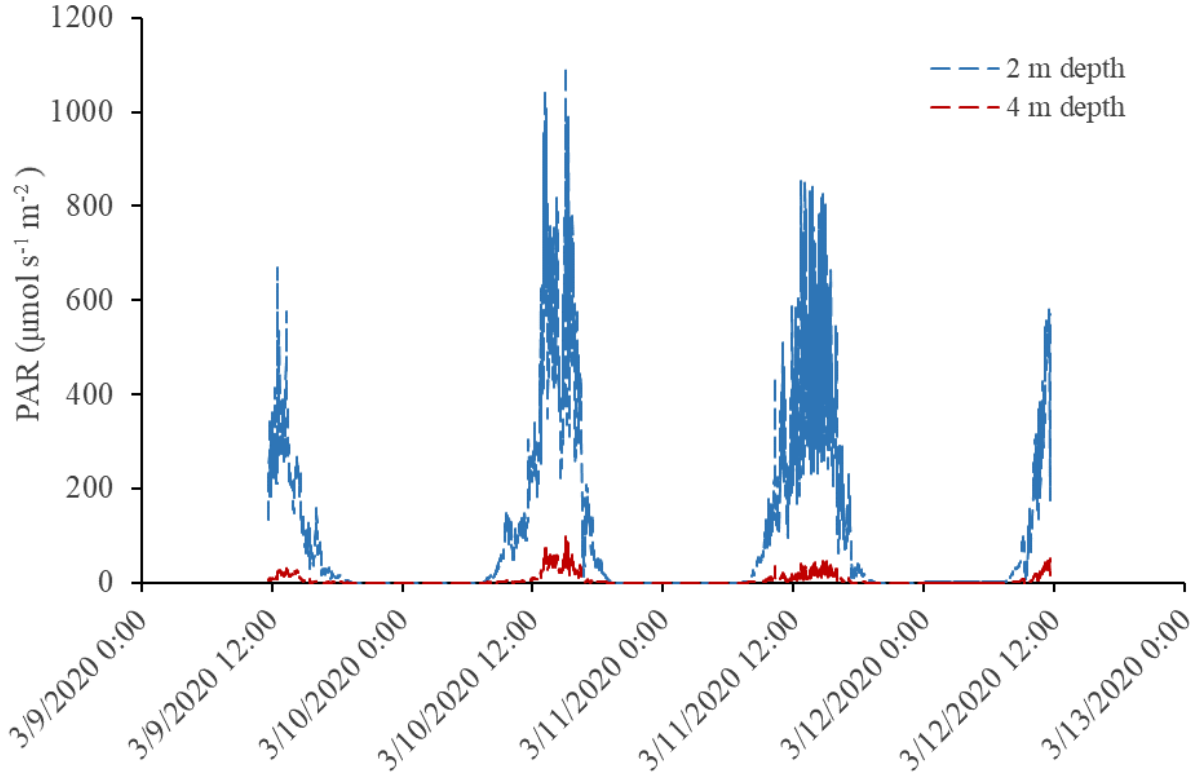

Figure 27. Galveston Channel PAR measurements, recorded at 2 and 4m depths, from 03/09/20 – 03/12/20.

The time-dependent uranium loadings at 2 m depth during the third deployment period (03/02/20 - 03/30/20) are shown in Figure 28. Before analysis, all braid snips were carefully rinsed to remove sediments. The 28-day apparent uranium loading level in the braid deployed at 2 m is 2.25 g U/kg_{ads}. Note that this "apparent" uranium loading is the detected uranium content from braid snips, which were exposed to seawater with low salinity (20.1 psu). After salinity correction to 35 psu and biofouling correction (0.3×28d/42d), the 28-day uranium loading level in the braid deployed at 2 m is consistent with the predicted curve (20 °C) shown in Figure 28. It is impressive because the braid was exposed to unfiltered seawater in the field, a real ocean deployment. Moreover, it is significantly higher than our testing data in PNNL–MCRL's raceway system (Table 5, the large LCW braids = 1.17 g U/kg_{ads}). However, the MCRL raceway testing was conducted under 10.8 ºC with 40 μm filtered Sequim Bay seawater. Therefore, the enhanced adsorption loading may be attributed to the warm seawater temperature in March (20.1 ºC) in the Galveston, TX site.

Hurricanes in the summertime also created problems for our experiments. In TAMUG's first deployment period (9/12/19 – 10/10/19), we experienced the Tropical Storm Imelda (landed TX on 9/17/19), a storm that caused devastating and record-breaking floods in southeast TX. Flooding on lands introduced significant inputs of freshwater to Galveston Bay. Both seawater temperature and salinity in the deployment site dropped significantly. The very low pH (6–7) was measured after the Tropical Storm Imelda and lingered for more than two weeks, pointing to the strong inputs of freshwater. Similarly, during TAMUG's fifth deployment period (08/19/20 – 09/16/20), Hurricane Laura (08/20 – 08/29/2020) also affected our experiments during this deployment.

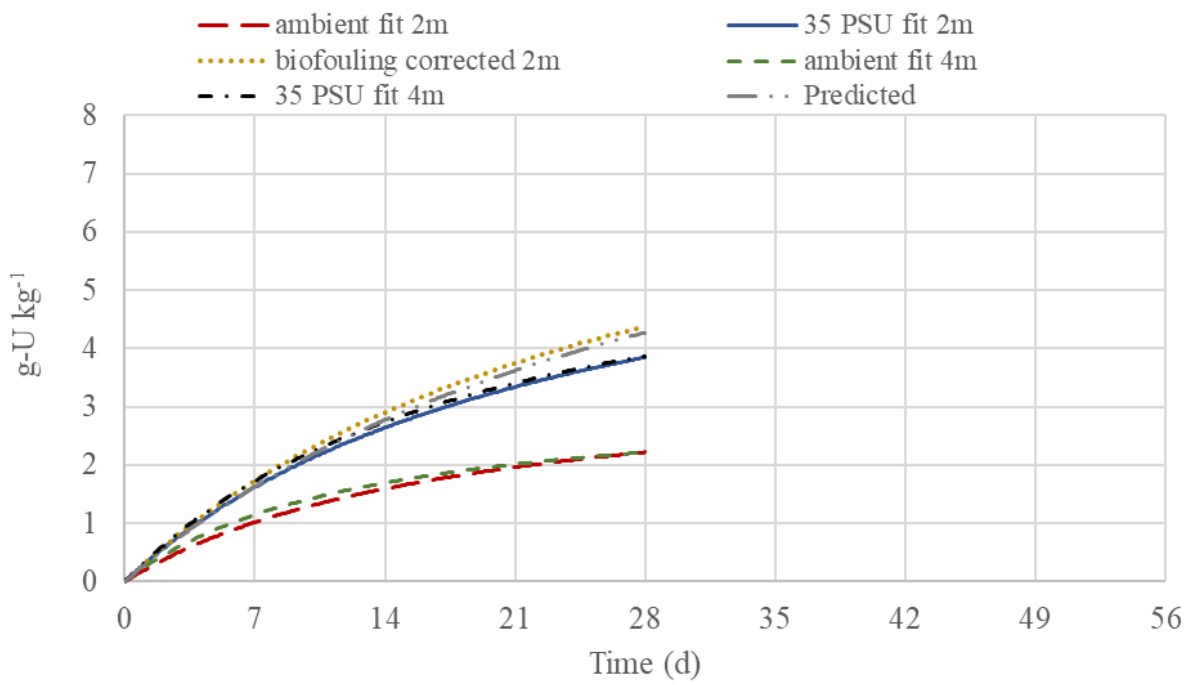

Figure 28. Uranium adsorption on the LCW-TW3c fiber during the third deployment period (03/02/20 - 03/30/20) in Galveston Channel.

VIII. Cost Analysis

LCW Supercritical Technologies started working with Dr.'s Erich Schneider and Margaret Byers at the University of Texas at Austin in 2017 to conduct techno-economic analyses of the use of the LCW adsorbent for extraction of uranium from seawater on a commercial scale. The details of their cost analysis approach are given in the literatures.[61, 62] Major parameters considered in determining the production cost of uranium from seawater include, adsorption capacity, adsorption rate, water temperature, biofouling, and degradation of the adsorbent with use.

One attractive feature of the LCW fiber adsorbent is its relatively low cost of prodction. The starting material is easily available common acrylic fibers and the production process involves two rather simple chemical reactions. The manufacturing cost depends on the scale of production. At a large production scale, the cost to produce the fiber adsorbent is estimated to be about $10.5 per kilogram as shown in Figure 29.

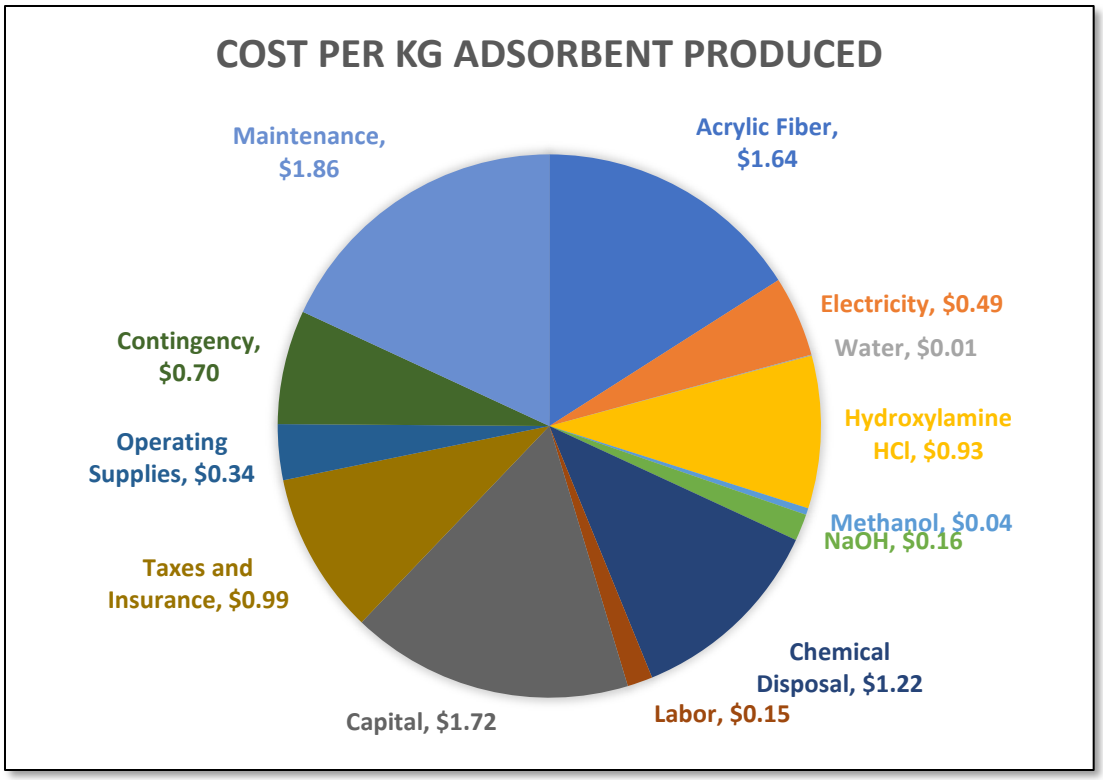

Figure 29. LCW fiber adsorbent manufacturing cost estimate ($10.50 per kilogram for 12,000 tons per year production).

The uranium adsorption capacities of the LCW adsorbent in seawater after 56 days of exposure is approximately 6 g U/kg adsorbent at 20 ºC. We have estimated the adsorption capacities of the LCW fiber at different seawater temperatures based on the van't Hoff equation and an enthalpy of adsorption of 57 kJ mol^{-1}.[8] Our estimated uranium adsorption capacities at 30 ºC after 56 days of exposure to seawater is about 13 grams of uranium. The effect of this temperature effect on the production of uranium from seawater with the LCW adsorbent is shown in Figure 30.

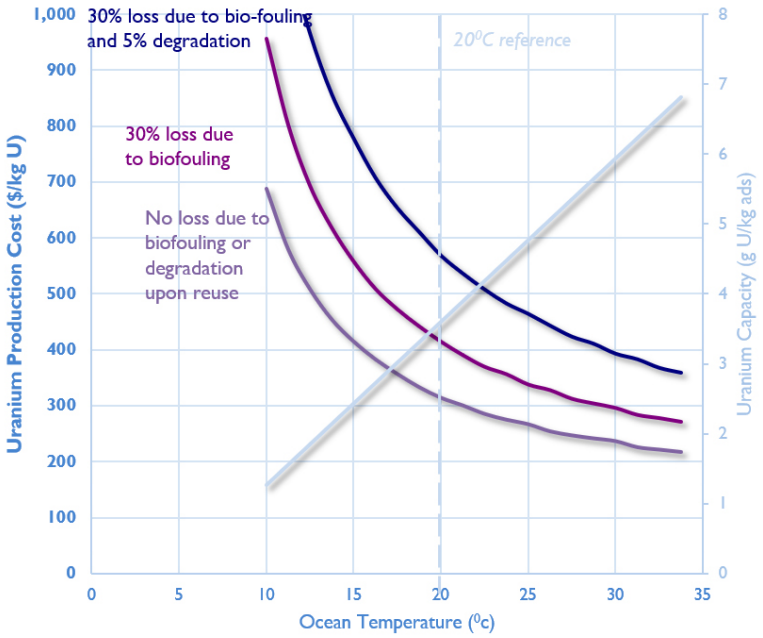

Figure 30. Uranium capacity and production cost of the LCW adsorbents as a function of temperature

A comparison of the cost to produce uranium from seawater using various adsorbents with varying operational conditions compared to terrestrial mining is shown in Figure 31. The production cost of uranium from seawater by amidoxime-based adsorbents is highly influenced by adsorption capacity, durability (number of re-uses) and the effect of temperature on adsorption capacity. This techno-economic analysis shows that the cost to produce uranium from seawater with the LCW adsorbent at 20 ºC is in the range of $280-460/kg U. When the seawater temperature is at 30 °C, the production cost is between $180-280/kg U. The current uranium spot market price is about $33/kg U. The fiber adsorption technology appears economically unfavorable at the present time for production of uranium from seawater. However, if other critical materials and precious metals discussed in Section *IV-B* could be recovered as by-products of the uranium extraction process, it might reduce the cost of uranium production from seawater. Further studies are necessary to explore this possibility.

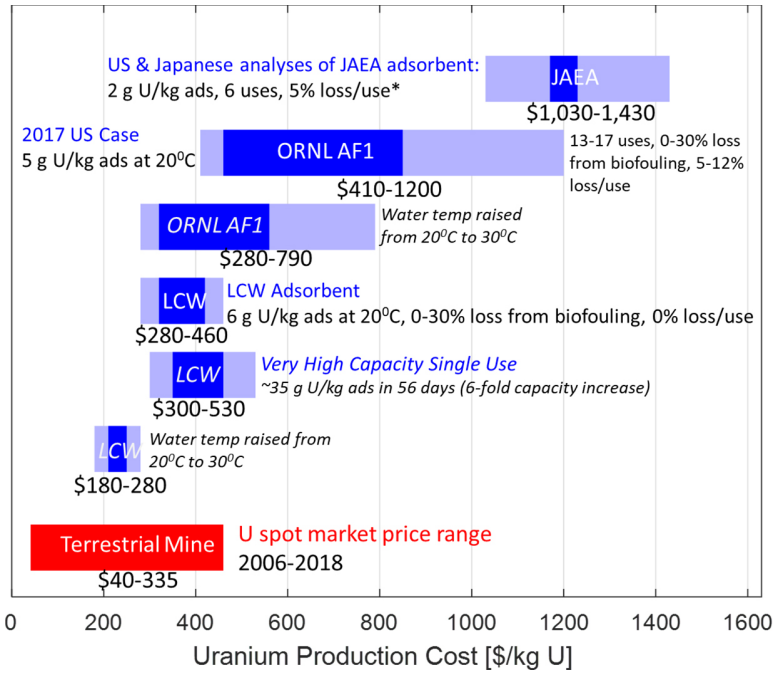

Figure 31. Seawater uranium production cost progression and potential milestones. (Updated from Industrial and Engineering Chemistry Research, 2013, Vol. 53, P.6076)[59]. *JAEA data from Science and Global Security, 2013, Vol 21, p134.[47]

Cost analysis for production of uranium from seawater depends on many factors. The analysis shown in Figure 31 does not represent a full bottom-up analysis of production costs for the LCW adsorbent, nor is it optimized in the sense that it uses off-the-shelf prices for the acrylic substrate and other commodities. The cost analysis was performed based on small scale laboratory observations and simple assumptions. In real marine environment, the effects of biological processes on uranium adsorption could be a major factor lowering the uranium adsorption rate or capacity. In our laboratory circulating flume studies, the effects of biofouling and organic matters on uranium adsorption are low compared with the Galveston Bay real marine environment tests. In the Galveston Bay experiments, the braids were often found to have algae and seaweeds attached to the fiber surface after a couple of weeks of exposure to the marine water environment. This phenomenon could affect the observed uranium adsorption results. Perhaps a scaled-up study in a remote coastal marine environment with little human activities would provide more realistic data to evaluate technical and economic feasibility for large scale production of uranium from seawater.

Developing very high-capacity fiber adsorbent is another approach to reduce cost of uranium production from seawater. The commercially available acrylic fiber used in this study has fiber diameters in the range of 20-25 microns. If adsorption of uranium occurs on the surface of the fiber adsorbent, then utilizing high surface area fiber adsorbent would increase uranium adsorption capacity. This high surface area fiber material idea may be achieved by using smaller diameters of acrylic fibers as starting material. For example, reduction of fiber diameter by a factor of 2 should double the surface area of the fiber on per unit fiber mass basis. Thus, reducing acrylic

fiber diameter from 20 microns to 5 microns would increase the total surface area of the fiber by a factor of 4 on a per gram fiber basis. The increase in starting material surface area could significantly improve the uranium adsorption capacity of the resulting fiber adsorbent. Research in this area is currently in planning.

Summary

Acrylic fiber can be chemically converted to an amidoxime and carboxylate containing chelating adsorbent for extraction of uranium from seawater. The seawater uranium adsorption experiments were performed at the Pacific Northwest National Lab's Marine and Coastal Research Lab (PNNL–MCRL) located in Sequim, Washington. Conversion of nitrile groups in acrylic fiber to amidoxime and carboxylate groups involves a two-step sequential reaction process, i.e., amidoximation using hydroxylamine followed by carboxylation with NaOH. At optimized ratios of amidoxime:carboxylate:nitrile (45%:45%:10%), the chelating fiber shows a higher uranium and lower vanadium adsorption capacity in seawater flow through column tests relative to other similar types of chelating fibers reported in the literature. Subsequent tests utilizing a circulating seawater flume system with braids made of ~10 grams of the fiber adsorbent confirmed the initial column test results. The uranium adsorption capacity of the braid reached 6.02 grams uranium per kg of adsorbent after 56 days of exposure in the seawater at 20 ^{o}C and the uranium/vanadium adsorption ratio remained close to unity. Using the one-site ligand saturation model, the estimated saturation capacity of uranium in seawater is about 7.73 grams per kg of adsorbent. The half-saturation time (15.7 days) is also shorter than those reported (>20 days) for the radiation-induced grafting produced amidoxime-containing fibers.[18-20, 44]

FTIR and NMR spectroscopy were used to characterize the fiber adsorbent. Solid-state ^{13}C NMR indicates that the amidoxime groups formed in the fiber are mainly the branch-chain diamidoxime structure instead of the cyclic imide dioxime structure reported for other amidoxime/carboxylate containing fibers. The equilibrium distribution coefficient K_D of uranium (U concentration in fiber/U concentration in seawater) between the fiber and the Sequim Bay seawater is about 2×10^6 at 20 ^{o}C. The fiber is also effective for extraction of critical materials such as rare earth elements, cobalt, and precious metals including silver, platinum, and palladium from the seawater.

Prior to uranium elution, the fiber should be washed with 0.01 M HCl to remove calcium, magnesium, and alkali metals adsorbed by the fiber. Elution of uranium from seawater exposed fiber can be accomplished using 0.3 M hydrochloric acid at room temperature. About 98% of the adsorbed uranium can be removed from the fiber under this condition. After uranium elution, the fiber is washed with 0.5 M sodium hydroxide to remove organic matters. The fiber can be reused for uranium adsorption after the alkali treatment.

Scaled up tests utilizing a large raceway flume system (950 L volume) and kilogram quantity of fiber material were performed to evaluate uranium adsorbent behaviors of different sizes of fiber braids with a small-size group (about 10 grams each braid) and a large-size group (about 60 grams each braid) for 28 days of exposure at the ambient temperature of 10.8 ^{o}C. The small-size braids in the raceway experiment were found to consistently outperform the large-size braids with respect to uranium adsorption. The results suggest the potential inhomogeneous adsorbent quality when adsorbent size was scaled up. Adsorption modeling was used to simulate the performance of the acrylic fiber derived absorbent at higher temperatures and longer exposure times for comparison with other amidoxime/carboxylate containing fibers developed at Oak Ridge

National Lab (AF-1 and AI8). The LCW adsorbents outperform both AF-1 and AI8 at lower temperatures with respect to uranium adsorption, while matching their adsorption at higher temperatures.

The scaled-up uranium adsorption experiments also demonstrated that gram quantities of yellowcake can be produced from the seawater using the large raceway flume system. After acid elution of uranium from the exposed fibers, the acid solution was treated with a tri-n-butyl phosphate/hexane solution to concentrate the uranium in the organic phase. This was followed by an ammonium carbonate back-extraction to transfer uranium from the organic phase back to an aqueous phase. After the back-extraction, by heating the ammonium carbonate solution to boiling and under reflux condition, precipitation of ammonium uranyl carbonate $(NH_4)_4[UO_2(CO_3)_3]$ yellowcake occurred.

Direct warm seawater uranium adsorption experiments were conducted at Galveston, Texas in 2019–2020. The selected site was located at the East Pier near TAMUG (Texas A&M University Galveston) campus. Customized davits with extended arms were employed for the deployment of LCW fiber braids in the Galveston harbor seawater for the experiments. Biofouling, algae activity, and coating of suspended sediment particles have serious effects on the uranium adsorption capacity of the fiber in this location. Hurricane in the summertime also created problems for the experiment. During the winter months (average temperature 20 ^{o}C) when algae activity is low in the Galveston Harbor, the uranium adsorption capacity agreed with the predicted performance of the fiber observed in the controlled circulating flume systems at PNNL–MCRL. The Galveston experiment highlights the necessity to select stations that are not highly affected by proximity to land-based influences.

A techno-economic analysis shows that the cost to produce uranium from seawater with the LCW adsorbent at 20 ^{o}C is between $280–460 per kilogram of uranium. In warm seawater (e.g. 30 °C), the uranium production cost is estimated to be between $180–280/kg U. The current uranium spot market price is about $33/kg. The fiber adsorption technology is economically unfavorable at the present time for production of uranium from seawater. However, if other valuable metals such as vanadium, cobalt, and palladium could be recovered as by-products of the uranium extraction process, it might reduce the cost of uranium production from seawater. Further research is necessary to explore this possibility.

References

(1) Kim, J.; Tsouris, C.; Mayes, R. T.; Oyola, Y.; Saito, T.; Janke, C. J.; Dai, S.; Schneider, E.; Sachde, D., Recovery of Uranium from Seawater: a Review of Current Status and Future Research Needs. *Sep. Sci. Technol.* **2013,** 48, 367-387.

(2) Abney, C. W.; Mayes, R. T.; Saito, T.; Dai, S., Materials for the Recovery of Uranium from Seawater. *Chem. Rev.* **2017,** 117, 13935-14013.

(3) Parker, B. F.; Zhang, Z.; Rao, L.; Arnold, J., An overview and recent progress in the chemistry of uranium extraction from seawater. *Dalton Trans.* **2018,** 47, 639-644.

(4) Lindner, H.; Schneider, E., Review of cost estimates for uranium recovery from seawater. *Energy Economics* **2015,** 49, 9-22.

(5) Gill, G. A.; Kuo, L.-J.; Janke, C. J.; Park, J.; Jeters, R. T.; Bonheyo, G. T.; Pan, H.-B.; Wai, C.; Khangaonkar, T.; Bianucci, L.; Wood, J. R.; Warner, M. G.; Peterson, S.; Abrecht, D. G.; Mayes, R. T.; Tsouris, C.; Oyola, Y.; Strivens, J. E.; Schlafer, N. J.; Addleman, R. S.; Chouyyok, W.; Das, S.; Kim, J.; Buesseler, K.; Breier, C.; D'Alessandro, E., The Uranium from Seawater Program at the Pacific Northwest National Laboratory: Overview of Marine Testing, Adsorbent Characterization, Adsorbent Durability, Adsorbent Toxicity, and Deployment Studies. *Ind. Eng. Chem. Res.* **2016,** 55, 4264-4277.

(6) Pan, H. B.; Liao, W. S.; Wai, C. M.; Oyola, Y.; Janke, C. J.; Tian, G. X.; Rao, L. F., Carbonate-H_2O_2 Leaching for Sequestering Uranium from Seawater. *Dalton Trans.* **2014,** 43, 10713-10718.

(7) Haji, M. N.; Drysdale, J. A.; Buesseler, K. O.; Slocum, A. H., Results of an Ocean Trial of the Symbiotic Machine for Ocean uRanium Extraction. *Environ. Sci. Technol.* **2019,** 53, 2229-2237.

(8) Kuo, L. J.; Gill, G. A.; Tsouris, C.; Rao, L. F.; Pan, H. B.; Wai, C. M.; Janke, C. J.; Strivens, J. E.; Wood, J. R.; Schlafer, N.; D'Alessandro, E. K., Temperature Dependence of Uranium and Vanadium Adsorption on Amidoxime-Based Adsorbents in Natural Seawater. *Chemistryselect* **2018,** 3, 843-848.

(9) Pan, H. B.; Wai, C. M.; Kuo, L. J.; Gill, G.; Tian, G. X.; Rao, L. F.; Das, S.; Mayes, R. T.; Janke, C. J., Bicarbonate Elution of Uranium from Amidoxime-Based Polymer Adsorbents for Sequestering Uranium from Seawater. *Chemistryselect* **2017,** 2, 3769-3774.

(10) Kuo, L. J.; Pan, H. B.; Wai, C. M.; Byers, M. F.; Schneider, E.; Strivens, J. E.; Janke, C. J.; Das, S.; Mayes, R. T.; Wood, J. R.; Schlafer, N.; Gill, G. A., Investigations into the Reusability of Amidoxime-Based Polymeric Adsorbents for Seawater Uranium Extraction. *Ind. Eng. Chem. Res.* **2017,** 56, 11603-11611.

(11) Pan, H.-B.; Kuo, L.-J.; Wood, J.; Strivens, J.; Gill, G. A.; Janke, C. J.; Wai, C. M., Towards Understanding KOH Conditioning of Amidoxime-based Polymer Adsorbents for Sequestering Uranium from Seawater. *RSC Advances* **2015,** 5, 100715-100721.

(12) Endrizzi, F.; Rao, L. F., Chemical Speciation of Uranium(VI) in Marine Environments: Complexation of Calcium and Magnesium Ions with [(UO2)(CO3)(3)](4-) and the Effect on the Extraction of Uranium from Seawater. *Chem.-Eur. J.* **2014,** 20, 14499-14506.

(13) Davies, R. V.; Kennedy, J.; Hill, K. M.; Mcilroy, R. W.; Spence, R., Extraction of Uranium from Sea Water. *Nature* **1964,** 203, 1110-1115.
(14) Astheimer, L.; Schenk, H. J.; Witte, E. G.; Schwochau, K., Development of Sorbers for the Recovery of Uranium from Seawater .2. The Accumulation of Uranium from Seawater by Resins Containing Amidoxime and Imidoxime Functional-Groups. *Sep. Sci. Technol.* **1983,** 18, 307-339.
(15) Schenk, H. J.; Astheimer, L.; Witte, E. G.; Schwochau, K., Development of Sorbers for the Recovery of Uranium from Seawater .1. Assessment of Key Parameters and Screening Studies of Sorber Materials. *Sep. Sci. Technol.* **1982,** 17, 1293-1308.
(16) Wang, C. Z.; Lan, J. H.; Wu, Q. Y.; Luo, Q.; Zhao, Y. L.; Wang, X. K.; Chai, Z. F.; Shi, W. Q., Theoretical Insights on the Interaction of Uranium with Amidoxime and Carboxyl Groups. *Inorg. Chem.* **2014,** 53, 9466-9476.
(17) Rao, L., *Recent International R&D Activities in the Extraction of Uranium from Seawater*. 2010.
(18) Das, S.; Oyola, Y.; Mayes, R. T.; Janke, C. J.; Kuo, L.-J.; Gill, G.; Wood, J. R.; Dai, S., Extracting Uranium from Seawater: Promising AF Series Adsorbents. *Ind. Eng. Chem. Res.* **2016,** 55, 4110-4117.
(19) Das, S.; Brown, S.; Mayes, R. T.; Janke, C. J.; Tsouris, C.; Kuo, L. J.; Gill, G.; Dai, S., Novel poly(imide dioxime) sorbents: Development and testing for enhanced extraction of uranium from natural seawater. *Chem. Eng. J.* **2016,** 298, 125-135.
(20) Das, S.; Oyola, Y.; Mayes, R. T.; Janke, C. J.; Kuo, L.-J.; Gill, G.; Wood, J. R.; Dai, S., Extracting Uranium from Seawater: Promising AI Series Adsorbents. *Ind. Eng. Chem. Res.* **2016,** 55, 4103-4109.
(21) Suzuki, T.; Saito, K.; Sugo, T.; Ogura, H.; Oguma, K., Fractional Elution and Determination of Uranium and Vanadium Adsorbed on Amidoxime Fiber from Seawater. *Anal. Sci.* **2000,** 16, 429-432.
(22) Leggett, C. J.; Parker, B. F.; Teat, S. J.; Zhang, Z.; Dau, P. D.; Lukens, W. W.; Peterson, S. M.; Cardenas, A. J. P.; Warner, M. G.; Gibson, J. K.; Arnold, J.; Rao, L., Structural and spectroscopic studies of a rare non-oxido V(v) complex crystallized from aqueous solution. *Chemical Science* **2016,** 7, 2775-2786.
(23) Kelley, S. P.; Barber, P. S.; Mullins, P. H. K.; Rogers, R. D., Structural clues to UO_2^{2+}/VO_2^{2+} competition in seawater extraction using amidoxime-based extractants. *Chem. Commun.* **2014,** 50, 12504-12507.
(24) Ivanov, A. S.; Leggett, C. J.; Parker, B. F.; Zhang, Z. C.; Arnold, J.; Dai, S.; Abney, C. W.; Bryantsev, V. S.; Rao, L. F., Origin of the unusually strong and selective binding of vanadium by polyamidoximes in seawater. *Nature Communications* **2017,** 8, 1560.
(25) Lashley, M. A.; Ivanov, A. S.; Bryantsev, V. S.; Dai, S.; Hancock, R. D., Highly Preorganized Ligand 1,10-Phenanthroline-2,9-dicarboxylic Acid for the Selective Recovery of Uranium from Seawater in the Presence of Competing Vanadium Species. *Inorg. Chem.* **2016,** 55, 10818-10829.

(26) Tian, G. X.; Teat, S. J.; Zhang, Z. Y.; Rao, L. F., Sequestering uranium from seawater: binding strength and modes of uranyl complexes with glutarimidedioxime. *Dalton Trans.* **2012,** 41, 11579-11586.
(27) Tian, G. X.; Teat, S. J.; Rao, L. F., Thermodynamic studies of U(VI) complexation with glutardiamidoxime for sequestration of uranium from seawater. *Dalton Trans.* **2013,** 42, 5690-5696.
(28) Kobuke, Y.; Tanaka, H.; Ogoshi, H., Imidedioxime as a Significant Component in So-Called Amidoxime Resin for Uranyl Adsorption from Seawater. *Polym. J.* **1990,** 22, 179-182.
(29) Brown, S.; Yue, Y.; Kuo, L.-J.; Mehio, N.; Li, M.; Gill, G.; Tsouris, C.; Mayes, R. T.; Saito, T.; Dai, S., Uranium Adsorbent Fibers Prepared by Atom-Transfer Radical Polymerization (ATRP) from Poly(vinyl chloride)-co-chlorinated Poly(vinyl chloride) (PVC-co-CPVC) Fiber. *Ind. Eng. Chem. Res.* **2016,** 55, 4139-4148.
(30) Brown, S.; Chatterjee, S.; Li, M. J.; Yue, Y. F.; Tsouris, C.; Janke, C. J.; Saito, T.; Dai, S., Uranium Adsorbent Fibers Prepared by Atom-Transfer Radical Polymerization from Chlorinated Polypropylene and Polyethylene Trunk Fibers. *Ind. Eng. Chem. Res.* **2016,** 55, 4130-4138.
(31) Pan, H.-B.; Kuo, L.-J.; Wai, C. M.; Miyamoto, N.; Joshi, R.; Wood, J. R.; Strivens, J. E.; Janke, C. J.; Oyola, Y.; Das, S.; Mayes, R. T.; Gill, G. A., Elution of Uranium and Transition Metals from Amidoxime-Based Polymer Adsorbents for Sequestering Uranium from Seawater. *Ind. Eng. Chem. Res.* **2016,** 55, 4313-4320.
(32) Abney, C. W.; Mayes, R. T.; Piechowicz, M.; Lin, Z.; Bryantsev, V. S.; Veith, G. M.; Dai, S.; Lin, W., XAFS investigation of polyamidoxime-bound uranyl contests the paradigm from small molecule studies. *Energy Environ. Sci.* **2016,** 9, 448-453.
(33) Sugasaka, K.; Katoh, S.; Takai, N.; Takahashi, H.; Umezawac, Y., Recovery of Uranium from Seawater. *Sep. Sci. Technol.* **1981,** 16, 971-985.
(34) Zhao, H. H.; Liu, X. Y.; Yu, M.; Wang, Z. Q.; Zhang, B. W.; Ma, H. J.; Wang, M.; Li, J. Y., A Study on the Degree of Amidoximation of Polyacrylonitrile Fibers and Its Effect on Their Capacity to Adsorb Uranyl Ions. *Ind. Eng. Chem. Res.* **2015,** 54, 3101-3106.
(35) Omichi, H.; Katakai, A.; Sugo, T.; Okamoto, J., A New Type of Amidoxime-Group-Containing Adsorbent for the Recovery of Uranium from Seawater. *Sep. Sci. Technol.* **1985,** 20, 163-178.
(36) Lin, W. P.; Lu, Y.; Zeng, H. M., Studies of the Preparation, Structure, and Properties of an Acrylic Chelating Fiber Containing Amidoxime Groups. *J. Appl. Polym. Sci.* **1993,** 47, 45-52.
(37) Mehio, N.; Williamson, B.; Oyola, Y.; Mayes, R. T.; Janke, C.; Brown, S.; Dai, S., Acidity of the Poly(acrylamidoxime) Adsorbent in Aqueous Solution: Determination of the Proton Affinity Distribution via Potentiometric Titrations. *Ind. Eng. Chem. Res.* **2016,** 55, 4217-4223.
(38) Smith, M., *March's advanced organic chemistry : reactions, mechanisms, and structure*. 7th edition / ed.; Wiley: Hoboken, New Jersey, 2013; p xxv, 2047 pages.
(39) Riva, E.; Gagliardi, S.; Mazzoni, C.; Passarella, D.; Rencurosi, A.; Vigo, D.; Martinelli, M., Efficient Continuous Flow Synthesis of Hydroxamic Acids and Suberoylanilide Hydroxamic Acid Preparation. *J. Org. Chem.* **2009,** 74, 3540-3543.

(40) Nyquist, R. A., *Interpreting Infrared, Raman, and Nuclear Magnetic Resonance Spectra*. Academic Press: San Diego, 2001.
(41) Socrates, G., *Infrared and Raman Characteristic Group Frequencies : Tables and Charts*. 3rd ed.; Wiley: Chichester ; New York, 2001.
(42) Pan, H. B.; Wai, C. M.; Kuo, L. J.; Gill, G. A.; Wang, J. S.; Joshi, R.; Janke, C. J., A highly efficient uranium grabber derived from acrylic fiber for extracting uranium from seawater. *Dalton Trans.* **2020,** 49, 2803-2810.
(43) Yuan, Y. H.; Zhao, S. L.; Wen, J.; Wang, D.; Gu, X. W.; Xu, L. L.; Wang, X. L.; Wang, N., Rational Design of Porous Nanofiber Adsorbent by Blow-Spinning with Ultrahigh Uranium Recovery Capacity from Seawater. *Adv. Funct. Mater.* **2019,** 29, 1805380.
(44) Kuo, L.-J.; Janke, C. J.; Wood, J. R.; Strivens, J. E.; Das, S.; Oyola, Y.; Mayes, R. T.; Gill, G. A., Characterization and Testing of Amidoxime-Based Adsorbent Materials to Extract Uranium from Natural Seawater. *Ind. Eng. Chem. Res.* **2016,** 55, 4285-4293.
(45) Deng, Y.; Ren, J.; Guo, Q.; Cao, J.; Wang, H.; Liu, C., Rare earth element geochemistry characteristics of seawater and porewater from deep sea in western Pacific. *Sci Rep-Uk* **2017,** 7, 16539.
(46) Kuo, L.-J.; Pan, H.-B.; Wai, C. M.; Byers, M. F.; Schneider, E. A.; Strivens, J. E.; Janke, C. J.; Das, S.; Mayes, R. T.; Wood, J. R.; Schlafer, N. J.; Gill, G. A., Investigations into the Reusability of Amidoxime-Based Polymeric Adsorbents for Seawater Uranium Extraction. *Ind. Eng. Chem. Res.* **2017,** 56, 11603-11611.
(47) Schneider, E.; Sachde, D., The Cost of Recovering Uranium from Seawater by a Braided Polymer Adsorbent System. *Science & Global Security* **2013,** 21, 134-163.
(48) Kuo, L. J.; Pan, H. B.; Strivens, J. E.; Schlafer, N.; Janke, C. J.; Wood, J. R.; Wai, C. M.; Gill, G. A., Assessment of Impacts of Dissolved Organic Matter and Dissolved Iron on the Performance of Amidoxime-Based Adsorbents for Seawater Uranium Extraction. *Ind. Eng. Chem. Res.* **2019,** 58, 8536-8543.
(49) Wood, J. R.; Gill, G. A.; Kuo, L. J.; Strivens, J. E.; Choe, K. Y., Comparison of Analytical Methods for the Determination of Uranium in Seawater Using Inductively Coupled Plasma Mass Spectrometry. *Ind. Eng. Chem. Res.* **2016,** 55, 4344.
(50) Kim, J.; Oyola, Y.; Tsouris, C.; Hexel, C. R.; Mayes, R. T.; Janke, C. J.; Dai, S., Characterization of Uranium Uptake Kinetics from Seawater in Batch and Flow-Through Experiments. *Ind. Eng. Chem. Res.* **2013,** 52, 9433-9440.
(51) Ladshaw, A.; Kuo, L. J.; Strivens, J.; Wood, J.; Schlafer, N.; Yiacoumi, S.; Tsouris, C.; Gill, G., Influence of Current Velocity on Uranium Adsorption from Seawater Using an Amidoxime-Based Polymer Fiber Adsorbent. *Ind. Eng. Chem. Res.* **2017,** 56, 2205-2211.
(52) Gill, G.; Kuo, L.-J.; Strivens, J.; J., W.; Schlafer, N.; Janke, C.; Das, S.; Mayes, R.; Saito, T.; Brown, S.; Tsouris, C.; Wai, C.; Pan, H.-B. *Summary of Adsorption Capacity and Adsorption Kinetics of Uranium and Other Elements on Amidoxime-based Adsorbents from Time Series Marine Testing at the Pacific Northwest National Laboratory*; Pacific Northwest National Laboratory: 2016.

(53) Ladshaw, A. P.; Wiechert, A. I.; Das, S.; Yiacoumi, S.; Tsouris, C., Amidoxime Polymers for Uranium Adsorption: Influence of Comonomers and Temperature. *Materials* **2017,** 10.
(54) Park, J.; Gill, G. A.; Strivens, J. E.; Kuo, L. J.; Jeters, R. T.; Avila, A.; Wood, J. R.; Schlafer, N. J.; Janke, C. J.; Miller, E. A.; Thomas, M.; Addleman, R. S.; Bonheyo, G. T., Effect of Biofouling on the Performance of Amidoxime-Based Polymeric Uranium Adsorbents. *Ind. Eng. Chem. Res.* **2016,** 55, 4328-4338.
(55) Wiechert, A. I.; Ladshaw, A. P.; Gill, G. A.; Wood, J. R.; Yiacoumi, S.; Tsouris, C., Uranium Resource Recovery from Desalination Plant Feed and Reject Water Using Amidoxime Functionalized Adsorbent. *Ind. Eng. Chem. Res.* **2018,** 57, 17237.
(56) Rehder, D., *Bioinorganic Vanadium Chemistry*. John Wiley & Sons: 2008.
(57) Sun, X. Q.; Xu, C.; Tian, G. X.; Rao, L. F., Complexation of Glutarimidedioxime with Fe(III), Cu(II), Pb(II), and Ni(II), the Competing Ions for the Sequestration of U(VI) from Seawater. *Dalton Trans.* **2013,** 42, 14621-14627.
(58) Parker, B. F.; Hohloch, S.; Pankhurst, J. R.; Zhang, Z.; Love, J. B.; Arnold, J.; Rao, L., Interactions of vanadium(IV) with amidoxime ligands: redox reactivity. *Dalton Trans.* **2018,** 47, 5695-5702.
(59) Kim, J.; Tsouris, C.; Oyola, Y.; Janke, C. J.; Mayes, R. T.; Dai, S.; Gill, G.; Kuo, L.-J.; Wood, J.; Choe, K.-Y.; Schneider, E.; Lindner, H., Uptake of Uranium from Seawater by Amidoxime-Based Polymeric Adsorbent: Field Experiments, Modeling, and Updated Economic Assessment. *Ind. Eng. Chem. Res.* **2014,** 53, 6076-6083.
(60) Silva Neto, J. B.; Urano de Carvalho, E. F.; Garcia, R. H. L.; Saliba-Silva, A. M.; Riella, H. G.; Durazzo, M., Production of uranium tetrafluoride from the effluent generated in the reconversion via ammonium uranyl carbonate. *Nucl Eng Technol* **2017,** 49, 1711-1716.
(61) Byers, M. F.; Schneider, E., Optimization of the Passive Recovery of Uranium from Seawater. *Ind. Eng. Chem. Res.* **2016,** 55, 4351-4361.
(62) Byers, M. F.; Schneider, E. In *Uranium from Seawater Cost Analysis: Recent Updates*, San Francisco, CA, June 11–15, 2017, Transactions of the American Nuclear Society: pp 85-88.

Appendix

Table A-1. The adsorption capacities of different elements on LCW fiber (Sequim Bay seawater at 20 ºC, 56 days exposure)

Elements	56-day Adsorption capacity ($g/kg_{ads.}$)	Elements	56-day Adsorption capacity ($g/kg_{ads.}$)
Mg	26.57	Pr	3.65×10^{-3}
Ca	14.80	Sc	2.27×10^{-3}
V	6.38	Ga	2.13×10^{-3}
U	6.02	Sn	2.05×10^{-3}
Fe	2.97	Cd	2.04×10^{-3}
Ni	2.95	Ho	1.56×10^{-3}
Zn	1.26	Eu	1.22×10^{-3}
Cu	0.44	Nb	1.17×10^{-3}
Ti	0.16	Tb	9.53×10^{-4}
Sr	0.13	Lu	7.19×10^{-4}
Mn	0.12	Tm	6.89×10^{-4}
Cr	0.22	Li	6.15×10^{-4}
Co	0.27	Ag	3.34×10^{-4}
Y	6.69×10^{-2}	Pt	9.88×10^{-5}
Zr	5.10×10^{-2}	Bi	9.28×10^{-5}
Mo	2.75×10^{-2}	Te	6.41×10^{-5}
La	1.91×10^{-2}	Sb	6.11×10^{-5}
Nd	1.87×10^{-2}	Th	5.23×10^{-5}
Ce	9.18×10^{-3}	Ir	4.33×10^{-5}
Dy	6.40×10^{-3}	Rh	8.51×10^{-6}
Pd	5.94×10^{-3}	Ru	7.06×10^{-6}
Gd	5.22×10^{-3}	Re	6.62×10^{-6}
Er	5.15×10^{-3}	In	6.61×10^{-6}
Yb	4.57×10^{-3}	Os	2.96×10^{-6}
Sm	4.18×10^{-3}		

*Average of 2 fiber braids (triplicate samples from each braid) about 10 grams each in a circulating seawater flume at MCRL

Table A-2. The range of distribution coefficient (K_D) of different elements on LCW fiber

Range of Distribution Coefficient (K_D)	Elements
10^8	Ir, Ti, Co
10^7	Pd, Ni, V, U, Fe, lanthanides
10^6	Cu, Zn, Mn, Cr, Y, Sn, Zr, Sc, Bi, Th, Pt, Ga, Os, Ru
10^5	Te, In, Nb, Ag
10^4	Rh
10^3	Mo
10^2	Re, Sb
10^1	Ca, Mg, Sr
$<10^1$	Li

Note: Values of $K_D > 10^4$ are considered to exhibit high affinity. Sequim Bay seawater at 20 ºC, 56 days exposure.